MODEL SOFT COLLOIDS OUT OF EQUILIBRIUM: GLASS-LIKE AND RE-ENTRANT TRANSITIONS

Dimitris Vlassopoulos[1], Emmanuel Stiakakis[2] and Michael Kapnistos[3]

[1]Foundation for Research and Technology – Hellas (FORTH),
Institute of Electronic Structure and Laser
and University of Crete, Department of Materials Science and Technology
Heraklion, Crete, Greece

[2] Forschungszentrum Jülich, Weiche Materie, Jülich, Germany

[3] DSM Research, Materials Science Centre, Geleen, The Netherlands

ABSTRACT

Star polymers with tunable number and size of arms, and thus interactions, represent ideal model systems for exploring the regime of soft material behaviour that interpolates between hard spheres and polymeric coils. This regime is characterized by a rich variety of properties that reflect the combination of polymeric and colloidal features. In this review we discuss some of these properties, and in particular the host of kinetic frustration phenomena encountered with such ultrasoft particles. They include soft colloidal glass-like transitions (a kind of jamming), induced upon increasing volume fraction (by heating or increasing the mass concentration), and the glass melting upon application of thermal (depletion) forces.

KEYWORDS: Soft colloids, glass transition, star polymers, jamming, depletion

1. JAMMING: A CHALLENGE IN SOFT MATTER RESEARCH

In the last two decades we have witnessed the emergence of soft condensed matter physics [1-14] as an interdisciplinary field of science, addressing fundamental research problems and having widespread technological applications. One of the foremost challenges in this area is exploring the potential universality in properties of different classes of soft materials [4, 5, 9, 10, 13-15]. As a particular example, theoretical and experimental works on complex fluids (ranging from polymers to surfactants and from colloids to granular materials) under conditions of high volume fractions have indicated the occurrence of a phenomenologically common feature, the so-called "jamming" [16]; it describes how different materials and external parameters (density, temperature, flow) can influence (enhance or eliminate) the ability of a system to flow [15-18]. The schematic jamming phase diagram of Fig. 1 provides a unified picture for the ergodic-to-nonergodic transition in a wide range of soft matter systems [15, 17, 18].

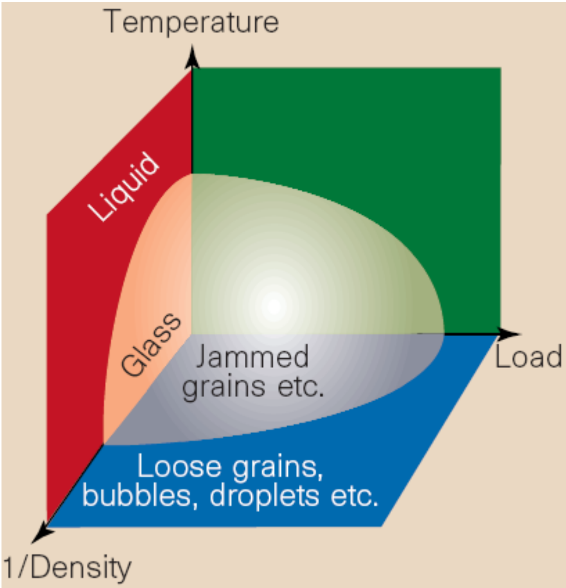

Figure 1: A possible phase diagram for jamming. The jammed region, near the origin, is enclosed by the depicted surface. The line in the temperature–load plane is speculative, and indicates how the yield stress might vary for jammed systems in which there is thermal motion. The region of main interest in this article is thet temperature-density diagram, whereas reference is made to the density-load region as well. Adapted from reference [15].

Some specific jamming situations (or kinetic frustration) include glass formation, gelation or shear thickening [19-30]. In fact, although the word "jamming" was originally preserved for stress-induced arrest in structured fluids [16, 18, 22, 24-30], arrest in the sense of frozen mobility can be induced by other means, i.e., without flow [15, 17, 18]; this is actually the subject of the present article. To put things in perspective, the nature of glass transition is one of the oldest unsolved problems in condensed matter physics [23, 31-36]. Experimental evidence (from rheological and diffusivity studies) suggests that in the dense state, colloids and polymers, two main representatives of soft matter, exhibit many similarities in the dynamic response (for example, solid-like behaviour, strong dependence of zero-shear viscosity or self diffusion coefficient on volume fraction). This, in conjunction with their sharp differences (size scales, type and range of order, origin of stress, to name a few) renders the detailed investigation of the intermediate range between these two limits necessary. To this end, a hard colloidal sphere with grafted polymer chains represents a typical intermediate system [37-39], that interpolates between the colloidal and polymeric limits: if many short chains are grafted, the colloidal nature prevails whereas for a few very long chains the polymeric response is dominant. Alternatively, micelles formed by block copolymers in selective solvents also serve as tunable colloidal particles, depending on the composition of the block copolymer. Among the many other possibilities for tuning the softness, and thus behaviour of particles, manipulation of microgels (via pH or temperature and/or solvent quality) has received a great deal of attention. In section 3 below, we present a very brief literature review on these three classes of soft colloidal systems (grafted particles, micelles, microgels).

Colloidal star polymers, i.e., stars with large number of arms f (functionality) are now established as a novel class of model soft colloidal systems with behaviour between linear polymeric chains and hard colloids [40-43]; the former case corresponds to $f = 1,2$ and the latter to high functionalities ($f \to \infty$). In fact, their wide-ranging weak repulsive potential [42, 44] is monitored by the number and size of the arms, as discussed below. They are characterized by a nonuniform monomer density profile (see Fig. 3 below) and can be thought of as ultrasoft colloidal spheres with a very small deformable core and a corona consisting of grafted chains (arms) [40, 43-46]. In these systems the polymeric and colloidal features, which influence their dynamic response, have been identified and relate primarily to arm (or arm segment) collective relaxation [47-49] and overall star self-diffusion [47-50], respectively. Their interplay reflects the various possibilities for designing and controlling such hybrid soft materials with the aim to achieve desired properties.

In this review, we present some intriguing properties of dense suspensions of colloidal stars, which are in fact universal for systems exhibiting very soft interaction pair potentials. We show the rich variety of kinetic arrest phenomena one can explore by tuning this kind of potential at molecular level, and thus shed light on the mechanisms of dynamic arrest (such as colloidal glass transition). More specifically, we focus our attention on two problems associated with colloidal stars: (i) their reversible thermal vitrification, and (ii) the effect of added depletion agents on their dynamic state.

2. A PICTURE OF DENSE SOFT COLLOIDS

The main issue when considering dense systems is that of topological constraints a given object feels due to its neighbours. For the present discussion we consider polymers and colloids. Concerning the former, say linear flexible chains in solution at very high volume fraction (φ) or in the melt, when the molecular mass is large enough, the topological constraints of the large number of neighbours

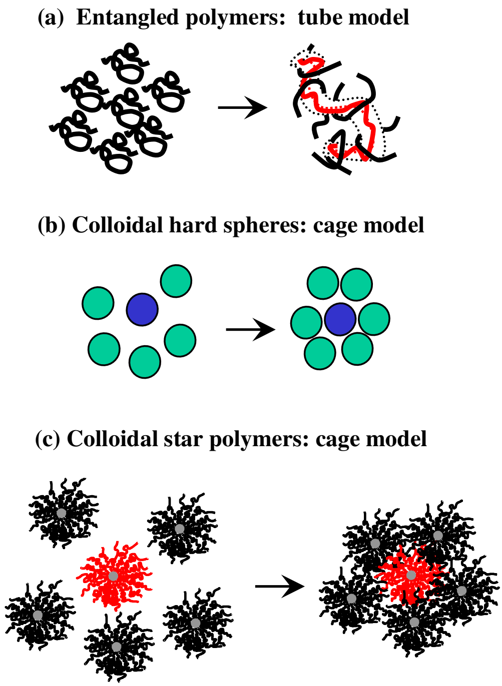

Figure 2: Schematic representation of crowded soft systems: entangled polymers **(a)**, colloidal hard spheres **(b)**, and colloidal star polymers **(c)**. The former are described by the tube model for entanglements, whereas the latter two by the general cage model for colloidal glasses.

(entanglements) confine a chain within a so-called tube [51-53], as illustrated in Fig.2a. The dynamics of this dense system are equivalent to the escape of the chain from its tube, the so-called reptation [51, 54]; this is treated within the mean field approach. On the other hand, when colloidal hard spheres reach a volume fraction of about 0.58, they form a glass [55]. In such a situation, a particle is constrained by its neighbours (a small number not exceeding 12) which restrict and eventually arrest its macroscopic motion (on the scale of its size), forming an effective cage [56-58], as illustrated in Fig. 2b. Local motions of the particle within its cage are of course possible (β -relaxation).

The so-called cage escape of the particle (α-relaxation) is the determining factor for the flow of the glass. Lastly, in the intermediate case of soft colloids, for example the colloidal stars, one can consider a modified cage effect: The terminal motion of the dense star suspension signalling macroscopic flow is that of the center of mass of the star [48-50]. The star is constrained within the cage of its neighbours; however, at the same time, due to their conformation (long arms) the stars interpenetrate forming effectively some entanglements of the outer blobs. It is necessary for the star to disengage from its neighbours (a process absent in hard spheres) and move its center of mass (cage escape) for macroscopic flow to occur. This is illustrated in Fig. 2c, and this interaction of the outer blobs of the stars has consequences on their properties. The latter modified cage situation brings analogies to attractive glasses, where a caged particle is bonded to some neighbours [59, 60]. Note however, that despite the similarities (also observed in the viscoelastic response [60, 61]), the physics in the two systems is not quite the same.

3. SHORT REVIEW OF SOME CLASSES OF SOFT COLLOIDS

3.1. Solid Particles with Grafted Polymer Chains

It is known that surfaces are often modified, typically by grafting polymeric layers, in order to control or alter the surface interactions. This methodology has reached a high degree of sophistication. For example, recently the use of copolymers has yielded responsive surfaces that can change a physical property (hydrophilicity, biocompatibility) upon an external trigger, such as temperature, pH, or salt concentration (polyelectrolytes). The grafting of polymers on surfaces leads to the formation of the so-called polymer brushes [62-67]. One important advantage of polymer brushes is their high degree of synthetic flexibility, particularly towards the introduction of a variety of functional groups. Brushes are commonly prepared by grafting polymers to surfaces, either via chemical bond formation between reactive groups on the surface and reactive polymer end groups, or by physi-sorption of (asymmetric) block copolymers with ‘sticky’ segments (or simply telechelic polymers) [63]. The grafted surfaces can be made of organic or inorganic materials. A recent concise review on the synthesis of polymer branches was presented by Edmondson et al. [68]. Moreover, in Ref. [69] and in the references therein one can find procedures for grafting of polymer chains (PS, PEO, PDMS) on oxide particles (SiO_2, TiO_2, Fe_2O_5, ZnO, Cr_2O_5), as well as PMMA and PEO chains on PS latex particles. Below, we focus on the grafting of nano- and micron-size solid particles.

Grafting of silica particles has been studied extensively. Several inverstigators [70-74] used PS or n-octadetyl chains grafted on silica particles in order to compare directly “soft” against equivalent “hard” sphere systems for studying depletion effects. In Ref. [70] the behavior of silica-g-PDMS systems was also investigated as a function of concentration. Similar grafting with PDMS was also carried out for the investigation of the effects of softness on the dynamic structure factor of concentrated suspensions in mixed solvents [75]. Stearyl alcohol was also used as a grafting layer to create model adhesive dispersions for studies of shear-induced structural changes [76, 77]. Along the same lines, Rueb and Zukoski [78, 79] investigated the flow properties of suspensions of silica particles with covalently bound n-octadetyl chains. Furthermore, Cawdery et al. [80] investigated SiO_2-g-PS and PS-g-PEO particles for stability in various environments (changing pH). Nommensen et al [37, 81] used silica particles with PDMS grafted chains as a model system to investigate the shear rheology of soft sphere suspensions. At about the same time, Mewis and co-workers [82] employed suspensions of silica particles with poly(butyl methacrylate) grafted chains and investigated the shear thickening effects as function of volume fraction. Temperature was proven a sensitive control parameter for changing the soft colloid volume fraction through the variation of the solvent quality [82, 83]. Green and Mewis [84] related the rheology with the wetting behavior of silica-g-PDMS spheres in PDMS matrix. They generated a phase diagram showing the stable and aggregating regions as a function of grafting density and free matrix polymer length, suggesting ways for obtaining the optimum grafting density of particles for stable suspensions [85]. Castaing et al. [86] measured the shear rheology of small (about 30nm in diameter) silica spheres with long grafted PDMS chains, in good solvent for PDMS and at different volume fractions.

PMMA latex particles have also served as a model colloidal system for many years. In fact, Pusey and co-workers employed PMMA coated with short hydroxy stearic acid (HSA) chains as model hard sphere systems [55, 56, 59, 87]. Along the same lines, Genz et al. [88] used the same model system and changed the core size and the degree of polymerization of the HSA corona chains in order to identify the interaction potential of soft spheres. In that way, the specific effects of the grafted polymers were explicitly taken into account through a hard core plus a soft tail potential. The question here is whether at short enough HSA length the grafted particle becomes truly a hard sphere. Despite the reported good comparison in the zero-shear viscosity data between bare silica and PMMA-HSA particles, which suggests an extended viscosity master curve [89], it turns out that the rheological behavior of grafted colloidal particles always deviates from that of true hard spheres, no matter how short the grafted layer is. This was recently studied in detail by Wagner and Mewis [90-92]. Note also that comparison between grafted and adsorbed chain have shown that the adsorbed chain particles have similar rheological behavior with chemically grafted particles [93].

Spherical polyectrolyte brushes constitute another versatile grafted colloidal model with tunable properties. A typical such system consists of a glassy polystyrene core onto which linear poly(acrylic acid) (PAA) or poly(styrene sulfonate) chains are chemically grafted. This system was studied in solution (mainly its size variation) by DLS (Dynamic Light Scattering) as a function of pH, ionic strength and valency of counterions [94, 95], as well as by viscosimetry [96]. Further details on the system's potential as a model colloid can be found in the reviews by Ballauff [97, 98] and the subsequent work [99-102] on the in-situ binding of proteins to spherical polyectrolyte brushes.

Several other combinations of particles and grafted layers have been proposed in the literature and used in conjunction with rheological studies. We only mention a few here. Aoki et al. [103, 104] probed the linear and non-linear rheology of ABS samples. The rubber particles had poly(styrene-co-acrylonitrile) chains grafted on their surface, at different composition. Fritz et al. [105] investigated colloidal systems consisting of PS-PBA particles with PMMA chains grafted; the focus of their work was the examination of the influence of pH, electrolyte concentration, and amount of polymer in the stabilizing layer on the stability and rheology of the dispersions. An interesting study on the reversible thermal gelation of PS particles with PEO grafted chains was presented by Shay et al. [106]; by changing the temperature and varying the solvent quality this soft colloidal suspension was shown to undergo a liquid-to-solid transition. Recently, Zackrisson et al. [107] studied the structure, dynamics and rheology of poly(ethylene glycol)-grafted polystyrene nanospheres in wide range from the liquid, ergodic to the glassy, non-ergodic regime. We close this section with a mention to the recent study of Bell et al. [108]. They utilized SiO_2-g-PMMA particles, where the polymer chains contained spirobenzopyran photochromic molecules; by the application of UV radiation, the stable suspensions underwent a transition causing a rapid aggregation.

The above brief discussion concerned spherical colloidal particles. Naturally, there is a huge literature on anisotropic colloidal particles, ranging from inorganic clay products to hybrids and from synthetic organic systems (e.g., block copolymers) to biological model particles (e.g., fd-virus). Refs. [109-121] provide a very small, partial account of the wide range of systems and behavior available.

3.2. Block Copolymer Micelles

Copolymers (diblock, triblock, etc) under appropriate conditions (use of selective solvent for one block) self-assemble into supramolecular structures, called micelles. The micelles most frequently take a cylindrical (worm-like) or spherical (star-like) shape, depending on the blocks composition, the latter shape being structurally very similar to stars [122-124]. To enhance the stability of the micelle (given the exchange kinetics of the aggregated copolymer chains [125]), the core is usually a crosslinked [126] or glassy material [127, 128]. The micelles are formed through a physical process, contrary to chemically grafted colloids or star polymers. This has the advantage that chemistry is simple and relatively inexpensive. A key disadvantage is the stability (due to the exchange kinetics), especially in cases of temperature variation. There are ways to overcome this difficulty, for example by crosslinking the core, say via UV radiation [126, 129, 130]. Recently, a versatile class of starlike poly(ethylene propylene)/poly(ethylene oxide) block copolymer micelles were introduced, that were stable due to a combination of high block incompatibility, kinetically frozen core and high interfacial tension between core and solvent [131]; furthermore, by using a co-solvent of varying composition, the aggregation number was controlled.

From the huge literature available on the subject, including a large variety of different materials that can be combined to create micelles, the different self-assembling capabilities of those systems (driven by combination of entropic and enthalpic interactions), and the tunability of their interactions, we select here a representative list with emphasis on their use in rheological investigations. The critical micelle concentration and aggregation number of diblock copolymer micelles were found to increase as the copolymer-solvent compatibility increased, and as the copolymer asymmetry increased [132]. The relative size of the corona to the core dictates, to a great extend, the order-disorder transition and phase diagram of micelles [133, 124, 134]. On the other hand, the solvent selectivity has made it possible to physically modulate the geometrical characteristics of the micelles, and thus their phase behavior [135-137]. This has lead to the utilization of several 'external' parameters for tuning micellar systems: The pH strength [138-140], the polymer/solvent concentration [141, 142] and the use of different solvents or matrices [143-145]. In addition, changing the temperature was found to be a particularly effective means for monitoring the micellar formation [146]. Alexandridis et al. [147-149], have reported very large numbers of micellar structures by adjusting the concentrations of two solvent plus copolymer systems. These results can lead to important applications as with relatively simple and easily accessible materials a large variety of structures can be achieved [150].

It has been demonstrated via the use of rheological measurements, that by tuning the relative core/corona size one can obtain a wide range of viscoelastic response, from polymeric to colloidal [151-153]. The colloidal character is typically attributed to the hard core and the polymeric character to the softer corona [154]. Cloitre et al. [155-156] have prepared micelles from triblock terpolymers. With appropriate solvent selection and concentration, bridge formation is promoted leading to elastomer blends with improved mechanical performance. Boudet et al. [157] have used thermosensitive block copolymer to control chemical crosslinking. By changing the temperature they were able to control the reactivity, creating a molecular switchable system.

Another development is the use of highly asymmetric block copolymers or end-functionalized polymers, which associate into micelles via electrostatic or hydrophobic interactions. Relative sizes are the key parameter controlling aggregation number and softness in a given solvent, and these systems exhibit a wealth of rheological proprties from liquid to crystal to kinetically arrested states [158-160].

Recent advances in interesting nanotechnological applications, such as templating and shape control with block copolymer micelles [161-163], the use and manipulation of block polyelectrolytes [140, 164, 165], the synthesis of doubly responsive (pH and salt) diblock and triblock copolymers [166] and the use of architecturally complex block copolymers [167, 168], suggest the potential of these systems as models for a wide range of technological problems. To this end, a better characterization and control of the achieved aggregation number and stability will be very helpful.

3.3. Microgel Particles

Microgel particles are cross-linked latex particles that are swollen in a good solvent. These particles are conveniently prepared by surfactant-free emulsion polymerization (SFEP) and may be viewed as sterically stabilized particles with or without a core [169]. The synthesis often suffers from poor particle size uniformity [170-175]. However, Saito and Ishizu [172] have reported an elegant approach for the synthesis of microgel particles, which is capable of producing nearly-monodisperse samples. The narrow particle size distribution combined with the inherent steric stabilization of the particles prepared by SFEP, makes them ideal model systems for the study of rheology and dynamics in solution. For instance, by changing the solvent quality the microgel particles swell or shrink. As a particular example, poly(N-isopropylacrylamide), abbreviated as PNIPAM, undergoes thermally induced low critical solution temperature, de-swelling when the solution temperature is increased above its LCST in water [173]; this is the most extensively studied water-swellable microgel system. The change of PNIPAM particle dimensions and internal structure (solvent or no solvent inside the particle) have of course direct influence in the intra- and the inter-particle interactions. This type of PNIPAM-response of colloidal particles to external stimuli has attracted significant attention lately, because of the enormous capabilities in applications [174, 175]. Another possibility for controlling size and softness variation in colloidal particles is by grafting PNIPAM microgels with poly(ethylene oxide) chains, yielding high grafting densities and eventually attraction of the densely grafted microgels, as the temperature increases [176].

The ionic microgel particles prepared to date frequently contain carboxylate groups derived from acrylic acid or methacrylic acid. Microgel particles containing these monomers swell at high pH [175]. On increasing the pH from low values to high values, the swelling extent increases as the (weak) carboxylic acid groups inside the microgel particles ionise. This effect may be described in terms of internal electrostatic repulsion or, equivalently, the osmotic contribution from mobile counter-ions in the ionic particles [177]. The particle swelling results in a substantial increase in the accessible segments for the microgel particle. The deformable nature of microgel particles has important implications for their rheological properties. Buscall [178] reported that the rheological behaviour of microgel particles is equivalent to that of hard particles with a thin, soft shell. The interaction between swollen microgel particles comprises contributions from steric and electrostatic terms, and this depends on the degree of crosslinking. In the fully swollen state, dispersions of microgel particles are intrinsically stable. As de-swelling occurs, the van der Waals forces become increasingly more significant and this has consequences on their structure and rheology [179, 180]. If charged groups are incorporated (in the surface or in the interior) into the particles during polymerization, then electrostatic interactions play a role in determining the stabilization.

Cloitre and co-workers [177, 181, 182] studied the rheology of polyelectrolyte microgels as a function of the physico-chemical environment (*p*H, ionic strength, degree of ionization), concentration and time. They found that their dynamics of polyelectrolyte micro-networks exhibit common features with both colloidal (polydisperse hard-sphere) suspensions and polymer gels. In terms of time dependence they found aging and rejuvenation phenomena similar to glassy colloidal systems. Additionally, these particles exhibited wall slip phenomena during flow [182].

A very promising microgel system for tuning softness and investigating rheological properties was studied in detail by Ballauff and Richtering. Concentrated colloidal dispersions of a core-shell latex with a PS core and a cross-linked, temperature-sensitive PNIPAM shell were investigated as a function of temperature and concentration. Below the transition temperature, the shell collapsed [183-191] and this had immediate effects on the viscosity of the dispersions. In fact, it was found that in the collapsed state, the dispersions behave similarly to hard-sphere suspensions (also yielding crystals and glasses), whereas in the swollen state they behave like soft colloids [186, 187, 192-194]; the PNIPAM crosslinking density also contributed to the softness of the overall particle, with interesting implications on the rheological properties [187, 192, 194-197]. It was also reported that it is possible to modulate the size of both the shell and the core independently with the use of both thermosensitive particle and polymer layers, yielding a rich phase diagram [184, 192, 197]. Note that, in swollen conditions and at high shear rates the shell is partially drained [196]. Aging effects have also been observed in microgel suspensions [181, 194] even in the swollen state (low mobility). Additionally, similar thermally responsive star-like microgels with potential for rheology studies have recently been synthesized (star block copolymers of PNIPAM and dimethylacrylamide) [198].

Recent use of nanoscopic microgel particles in nanocomposites revealed a host of intriguing phenomena, such as decrease of viscosity upon addition of the particles to the polymer matrix [199]; these effects confirm the importance of these systems as rheological research tools, but their description is beyond the scope of this article.

4. COLLOIDAL STAR POLYMERS AS MODEL SOFT SPHERES

Given the above developments, one may wonder why there is need (if any) for yet another model colloidal system, and further what makes the stars so unique. As this is a central point in this article, it does merit some attention. Actually, by looking at the available experimental evidence in the literature, one can realize the following facts:

Despite the wealth of systems available, with different softness, most systems are not so well characterized: polydipsersity, limited control of aggregation or grafting density, difficulty in reproducing exactly the same composite particle, particle stability (particularly with respect to time and to temperature). They are also heterogeneous in the sense that chemically different species are combined to form, say, a core-shell particle. On the other hand, their softness can be tuned by various external parameters, more notably temperature, pH, solvent and additives.

In addition, a proper microscopic description of the particles interaction potential is highly desirable. Related to this point, and given the complexity of interactions, model systems with as simple as possible, well-understood interactions, are needed: for example, no charges, no enthalpic, only entropic (excluded volume) interactions. It is a rather formidable task to account for all these factors quantitatively and at the same time tune the particle's softness (by varying the number and/or size of the 'grafted' chains) in a way that allows exploring the regime between the polymeric and hard colloidal limiting behaviours. As to the possible question whether all these factors matter, the answer depends to a large extent on what is at stake. From the point of view of understanding the fundamentals of the interrelation between interactions and properties, and thus eventually exploring the universality of behaviour and the degree to which it holds, these factors matter indeed. In particular, rheological properties are extremely sensitive to small differences in particles characteristics, stemming from such factors. As an example here, we iterate the deviation of the

PMMA-HSA particle viscosity from the true hard sphere behaviour, even when the HSA layer is tiny [89-93].

Colloidal star polymers are, in our view, ideal soft colloidal model systems, that resolve nearly all of the above uncertainties. Due to their synthesis procedure (high vacuum anionic polymerization), they are as monodisperse as possible [41]. They are homopolymers, with only excluded volume interactions, chemically and structurally homogeneous. Their softness is tuned by synthesis (number and size of arms) and/or temperature in different solvents. At the same time, they are stable, and they can also be functionalized in various ways [200]. Their only disadvantage, admittedly not an unimportant one, is their far nontrivial synthesis, which makes them not readily available [41]. But there can be a direct analytical description of the softness [42, 44, 45] and, therefore, they are indeed models for exploring important aspects of the physics and rheology of colloidal suspensions, and to this end we feel that they are important. At the same time, they offer possibilities for creative thinking in terms of methodologies for preparation of (improved) particles with similar performance [40-43, 201].

Multiarm 1,4-polybutadiene stars were synthesized by Roovers and co-workers via two distinct routes:

(i) using chlorosilane chemistry, central dendritic cores of spherical shape and different generations were synthesized, on which the desired number of polymeric arms were grafted [41, 202, 203]; for the present discussion we focus on such regular stars with nominal functionality, f=18-128 and nominal arm molecular mass M_a=10000-80000 g/mol (for the measured exact values of molecular weights and functionalities the reader is referred to Refs 41, 202, 203 and Table 1). Note that star polymers are distinctly different from dedrimers; the latter represent another class of model colloidal particles [46, 204, 205], not considered in this review.

(ii) a short 1,2-polybutadiene backbone chain was hydrosilylated with $HSi(CH_3)Cl_2$ yielding two coupling sites per monomer unit, which were substituted with 1,4-polybutadiene by addition of poly(butadienyl)lithium [206]; in the present article such irregular stars (without central spherical core) with nominal f=270 and M_a=11000-42000 g/mol are considered.

There have been alternative efforts for synthesizing star polymers of intermediate functionality (up to 36) [207, 208] or high functionality (up to 239) [209], but there are issues with their characterization (and ability to reach higher functionalities in the former case). In addition, limited studies with those stars have been reported [207-209]. Today, it is widely accepted that Roovers' stars are the best characterized, true model systems.

All star polymers obtained from the above procedure are nearly monodisperse with $M_w/M_n<1.1$ (M_w being the total weight average and M_n the total number average molecular masses), and their main molecular characteristics are listed in Table 1.

Code	*f*	M_wx10^6 (g/mol)	N_a (1)	R_g (nm) (2)
LS6	263	11.2	783	42.4
LS5	269	7.9	540	36.7
LS4	267	4.9	337	24.5
12880	122	8.8	1333	42.4
12856	127	5.95	870	34.5
12828	114	2.98	483	21.6
6480	59	4.2	1318	34.1
6460	61	2.89	880	28
6430	56	1.34	443	18.5
6415	60	0.725	224	12.7
6407	62	0.395	117	9.8
3280	34	3.01	1738	37.6
3237	35	1.33	768	22.4
3220	33	0.644	372	14.5
3216	32	0.558	322	13.4
3210	31	0.301	174	10
3718	18	0.762	778	19.9
2518	19	0.541	523	17.4
1518	18	0.311	318	12.4

Table 1: Molecular Characteristics of the 1,4-Polybutadiene Stars. Data taken from references [41, 202, 203, 206, 40, 43]. (1) Degree of polymerization per star arm. (2) From SANS measurements in dilute solution (in the good solvent methylcyclohexane).

Based on the Daoud-Cotton model [45], multiarm star polymers constitute effective core-corona particles with core radius $r_c \sim f^{1/2}$ and softness defined as $s = L/(L + r_c)$, L being the corona thickness [43, 47, 83]; typical value of s for the 128-arm stars is about 0.885 [210]. Fig. 3 illustrates a cartoon representation of a single multiarm star in a good solvent; the different shaded areas are meant to depict the density profile. Due to topology, the blob size increases with the radial distance and three monomer density regimes can be observed [43, 45, 211]: the melt-like core regime, the theta-like (or unswollen) regime, where the blobs are ideal and only solvent can penetrate in a dense suspension, and the excluded volume (or swollen) regime, where the blobs are swollen and star-star interpenetration can take place in dense suspensions. For details the reader is referred to Ref. 45. Note further, that the form factor, as measured by SANS in dilute solutions, can be analyzed using the Daoud-Cotton scaling as also done in the case of micelles [123, 124, 212]. From the extracted radius of gyration R_g (from SANS or SALS, the latter for larger systems, in dilute solutions) and hydrodynamic radius R_h (from DLS in dilute solution [47, 211]), in good solvent, the ratio R_h/R_g was found to increase slightly with functionality as follows [40, 43]: $R_h/R_g = 1.24$ for $f = 18$, 1.28 for $f = 32$, and 1.4 for $f = 64$ or 128. These values are consistent with the consideration of these stars as soft colloidal particles [40, 43].

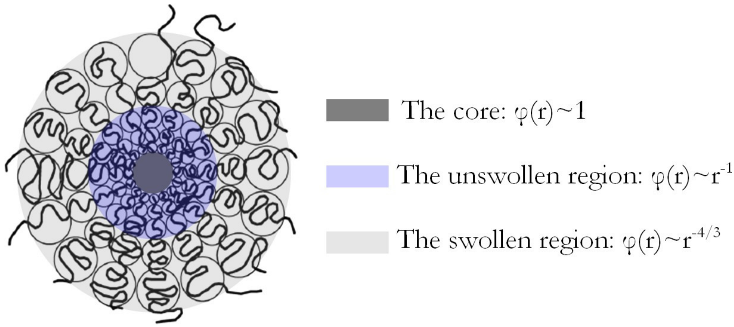

Figure 3: Schematic of a single colloidal star polymer (here with 16 arms) in good solvent, along with is monomer density profile φ(r). From the core to the periphery the three different regions, namely melt-like (core), ideal (unswollen) and excluded volume (swollen) region are depicted.

5. TUNING THE SOFTNESS: FROM POLYMER COILS TO HARD SPHERES

Recently, Likos et al. [44] have proposed an effective potential that describes the interaction between two stars. The idea is that for high functionality these systems are virtually spherical objects exhibiting a Yukawa type of interaction at long distances, typical for sterically stabilized colloids, whereas at short distances they feel a strong logarithmic repulsion. In the limit of low functionality they resemble polymer coils whereas in the other extreme of very high functionality they approach hard sphere behavior. Thus, the number of arms provides a means for tuning the star-star interaction from hard-sphere-like to polymer-like, which is solely based on excluded volume constraints. The potential $U(r)$ is given by (see also inset of Fig. 4) [44]:

$$\frac{U(r)}{k_B T} = \begin{cases} (5/18) f^{3/2} \left[-\ln(r/\sigma) + (1+\sqrt{f}/2)^{-1} \right] & \text{for } r \le \sigma \\ (5/18) f^{3/2} (1+\sqrt{f}/2)^{-1} (\sigma/r) \exp\left[-\sqrt{f}(r-\sigma)/2\sigma \right] & \text{for } r > \sigma \end{cases} \quad (1)$$

where σ is the effective corona diameter (e.g., $\sigma \propto f^{1/5} N_a^{3/5}$ for good solvents, N_a being the arm degree of polymerization) [40, 42, 45]. This strong variation of $U(r)$ is also reflected in the macroscopic properties of colloidal stars.

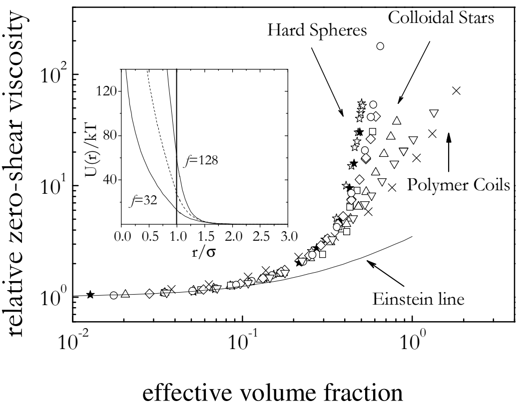

Figure 4: Relative zero-shear viscosity as function of the effective volume fraction (based on the hydrodynamic radius) for various soft systems: (1) hard spheres [(open star) poly(methylmethacrylate) in decalin, 640 nm diameter [213] (filled star) poly(methylmethacrylate) in decalin, 602 nm diameter [214]], (2) colloidal stars of 1,4-polybutadiene [215] [(○) LS6; (□) 12880; (◇) 12807, f = 128, M_a = 7000 g/mol; (△) 6407, f = 64, M_a = 7000 g/mol; (▽) 3280, f = 32, M_a = 80000 g/mol] and (3) linear chains (×) (1,4-polybutadiene, M = 165000 g/mol). See also Table 1. Data taken from reference [210]. The solid line is the Einstein prediction. Inset: Prediction for the star-star interaction potential of Likos et. al. [44] as a function of the normalized star-star distance (eq. 1). Functionality from right to left f = 32, 64, 128. Vertical line is the hard sphere potential.

A representative example is given in Fig. 4 which depicts the variation of the relative (to the solvent) zero-shear viscosity with the effective volume fraction (based on the hydrodynamic radius R_h) for stars of varying functionality [210, 215]. For comparison, reasonably well-understood data from hard spheres ($f \to \infty$) [213, 214], linear polymer solutions ($f = 1,2$) and an intermediate star functionality ($f = 32$) [215, 6] are also included. It is clear from this master plot that, as the functionality increases the colloidal stars tend toward hard sphere behaviour [216], whereas stars of low functionality behave as linear polymer coils [6].

Another manifestation of the internal structure of the stars is their ordering at high concentrations, a direct consequence of their excluded volume interactions on the star size scale. Despite theoretical predictions [42, 217-220] suggesting that crystallization takes place over a small concentration window around the star overlap (due to interplay of osmotic and elastic forces of the star arms), nearly all experimental observations indicate liquid-like order [221-225, 211, 212]. There is only fragmental information suggesting evidence of crystallization for stars with 128 arms, which were sheared prior to SANS measurements [224], as well as for larger but not so 'regular' and well-characterized stars [209]. This is a delicate issue that certainly needs further elaboration in the future. The star polymers investigated in the context of this review are listed in Table 1.

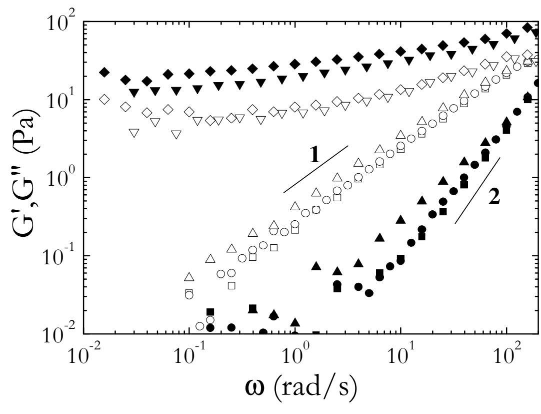

Figure 5: Dynamic frequency sweeps of 12880/decane 4.6 wt% solutions, indicating the thermal liquid-to-solid transition (□: 20°C, O: 25°C, Δ: 30°C, ∇: 33°C, ◊: 35°C. Solid symbols: G'; Open symbols: G''). Data taken from reference [225].

6. HEATING-INDUCED REVERSIBLE VITRIFICATION

6.1. The phenomenon

Recently, it was reported that concentrated solutions of colloidal stars in an intermediate solvent (where stars can swell with increasing temperature) undergo a reversible vitrification upon heating [211, 212, 225]. This counter-intuitive phenomenon was attributed to the formation of clusters of interpenetrating swollen stars, causing a dynamic arrest of the solution. The dramatic effect of temperature in inducing a liquid-to-solid transition is easily probed with simple rheological experiments. A characteristic example is shown in Fig. 5, where the storage (G') and loss (G'') moduli of a non-dilute star solution (4.6% wt of 12880 in decane) are plotted as function of frequency for various temperatures. At lower temperatures the polymer solution behaves like a viscous liquid, whereas at higher temperature it exhibits a solid-like response. The transition from a liquid-like terminal behavior with $G' \sim \omega^2$, $G'' \sim \omega$, $G'' > G'$ to an elastic solid-like response with $G' > G''$ exhibitng a very weak frequency dependence, is accompanied by a sharp enhancement of the moduli (especially G').

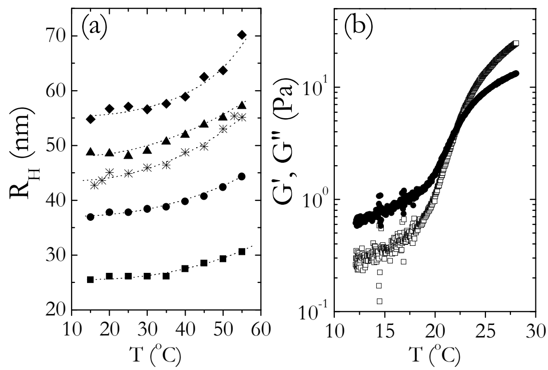

Figure 6: (a) Temperature dependence of the effective hydrodynamic radius R_h of stars in various solvents, as determined from dynamic light scattering measurements in dilute solutions (c<c*). (■: 12828/decane, ●: 12856/decane, ▲: 12880/decane, ◆: LS6/decane, *: 12880/tetradecane). The lines are drawn to guide the eye.

(b) Dynamic temperature ramp experiment for LS6/decane 5 wt% solution monitored at 5 rad/s, $1^{o}C/min$. Solid symbols: G″; Open symbols: G′. Data taken from references [211, 212].

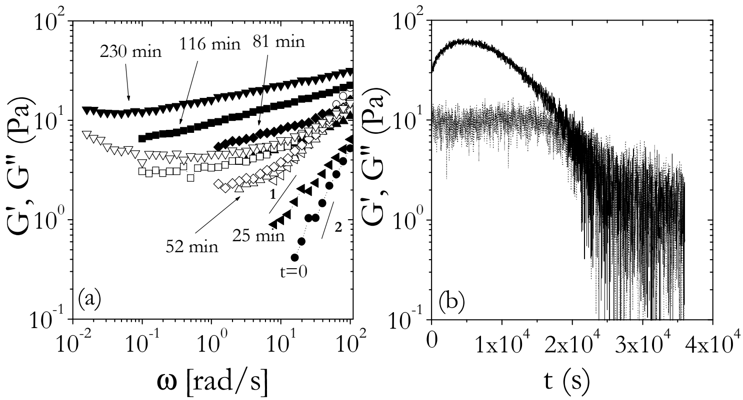

Figure 7: (a) Linear viscoelastic spectra (G′ , G″) of 12880/decane 5.2 wt% at 7°C (taken through a jump from about -10°C) and different times, demonstrating the long vitrification kinetics (o: original measurement at time t = 0 after the measurement temperature was reached; ◁: t = 25 min, Δ: t = 52 min, ◊: t = 81 min, □: t = 116 min, ∇: t = 230 min). Solid symbols: G″ ; Open symbols: G′

(b) Representative dynamic time sweep upon quenching 12880/decane 3.9 wt% to 20°C (from 45°C) at 1 rad/s, demonstrating the long time for fluidization experiment (solid-to-liquid). Data are taken from reference [212].

This effect is remarkably manifested in dynamic temperature ramps at low frequencies and heating rates (typically 1ºC/min), as demonstrated by the plot of Fig. 6b. Upon heating, the stars swell, as indicated by the increase of the hydrodynamic radius upon heating in a dilute star solution (Fig. 6a) [211, 212]. Note that the opposite effect is observed for low functionality stars (f < 32) and linear polymers, which exhibit the typical Arrhenius temperature dependence (moduli decreasing with temperature); in these cases swelling is insufficient to compensate for the classic liquid-state viscosity decrease [201].

Once the thermally-induced glassy state is formed, cooling to the initial temperature yields melting and eventually the initial viscous liquid is recovered. The kinetics of the glass formation (upon heating) and melting (upon cooling) processes are rather complex and not fully understood yet, but they are clearly characterized by relatively short glass formation times (around 2 hours, see for example Fig. 7a) and recovery times (which can exceed 10 hours, see for example Fig. 7b). Naturally, these times depend on the system, the concentration and the temperature difference.

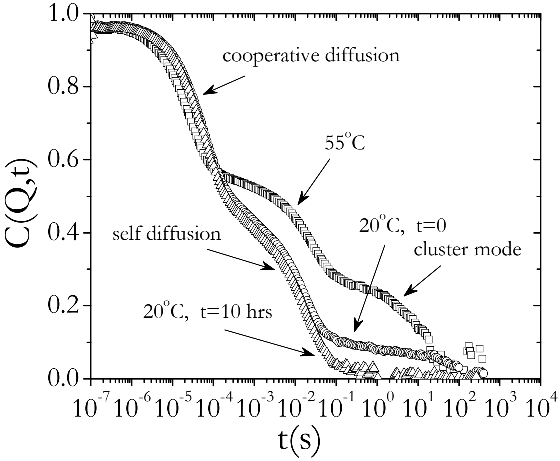

Figure 8: Normalized intermediate scattering function of 12856/decane 5.5 wt% at a value of the scattering wavevector Q=0.033 nm^{-1}, measured at 55°C in the solid (glassy) state and at different times upon subsequent cooling to 20°C in the liquid state. The various relaxation processes are indicated by arrows. Note that the solid state is characterized by the slow cluster mode which looses intensity upon cooling and eventually disappears when the equilibrium liquid is recovered (after 10h). Data taken from reference [212].

Independent DLS measurements provide useful information, in addition to the quantitative confirmation of these findings [212, 225]. In fact, they show that the high-temperature glassy state is associated with the presence of a slow mode, typically assigned to cluster formation [226-229]; this mode disappears upon melting of the glass [212]. A typical example is depicted in Fig. 8. Furthermore, the extracted typical average size from the moduli in the 'solid' regime (see for example Fig. 5), $\xi = \left(k_B T / G'\right)^{1/3}$, is slightly above the single-star R_h, conforming to the presence of some kind of larger entities (the clusters) [211, 212].

6.2. Interpretation

To interpret this phenomenon, the following mechanism has been postulated [211, 212, 225]: as the temperature increases, the solvent quality improves and the peripheral blobs of the interacting liquid-ordered soft spheres swell, yielding an

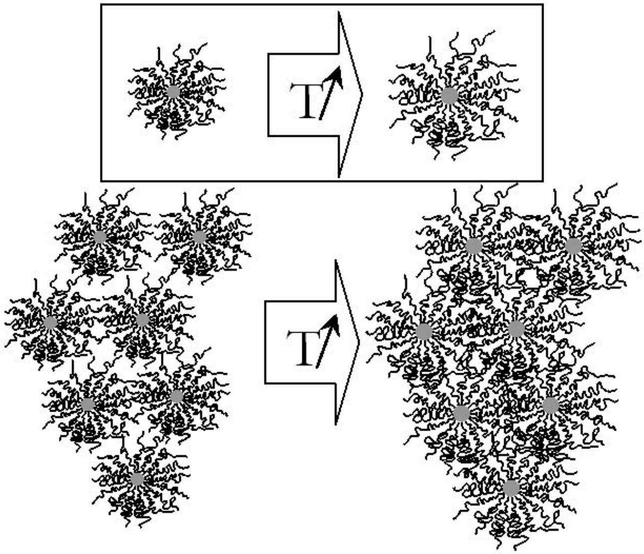

Figure 9: Cartoon representation of the heating-induced vitrification process. Single star swelling upon heating (top) and crowding of the swollen stars at high concentration.

enhanced overall size (see also cartoon of Fig. 9). Consequently, the stars increase their arms' overlap, but not to a large extent because of the strong excluded volume repulsions [42, 44]; at the same time, the star-star distance, is unaffected due to the overall incompressibility of the system [42, 217, 229], as confirmed by small angle neutron scattering (SANS) experiments (see for example the data of Fig. 10) [211, 212, 225]. This crowding eventually leads to a dynamic frustration (i.e., a form of jamming) of the stars due to the formation of clusters consisting of a few 'trapped' spheres, in equilibrium with 'free' spheres [19, 60, 211, 212].

The cartoon of Fig. 9 attempts at representing a snapshot of this situation. The single star swells upon heating (top). The respective concentrated star suspension (bottom) becomes more crowded as its effective volume fraction is increased, as also reflected in the areas of overlap. This kind of jamming leads to the macroscopic immobilization of the system. In addition, the present findings show how the effective volume fraction of these crowded soft systems can increase with temperature apart from density, offering new possibilities for dynamically arrested states. The star swelling affects the effective potential as well, and by accounting for its change it is

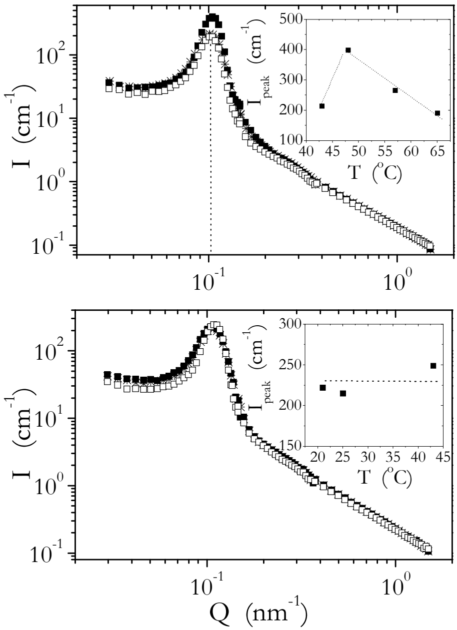

Figure 10: Double logarithmic plot depicting the SANS scattering intensity *I* versus the scattering wave vector Q for : **(a)** 12880/*d*-tetradecane 5.47 wt% at three temperatures 43°C (*; liquid), 48°C (■; liquid) and 65°C (□; glass); and **(b)** 12880/*d*-tetradecane 6.44 wt% at three temperatures 21°C (■; liquid), 25°C (*; glass), 43°C (□; glass). To appreciate the differences in two concentrations, see also the state diagram of Fig. 11 and the discussion in [211]. Insets: Temperature dependencies of the peak intensities I_{peak}. Lines are drawn to guide the eye. Data are taken from reference [211].

possible to predict the same qualitative trends, i.e., kinetic frustration upon heating; the latter is manifested as a long-time plateau in the star mean-squared displacement [229]. In addition to the DLS experiments, the presence of clusters was also detected with pulsed-field gradient NMR measurements, which probed a long-time non-relaxing plateau in the *S(Q,t)* and the mean-squared displacement [225, 50].

It appears, therefore, that the star arm expansion upon heating is responsible for the slow formation of long-lived clusters (the effective cages [4, 56, 57]), which involve some kind of cooperativity and kinetic arrest of the system, forming a solid, much like a glass (or gel) formation process [4, 229-234]. This observation is rather

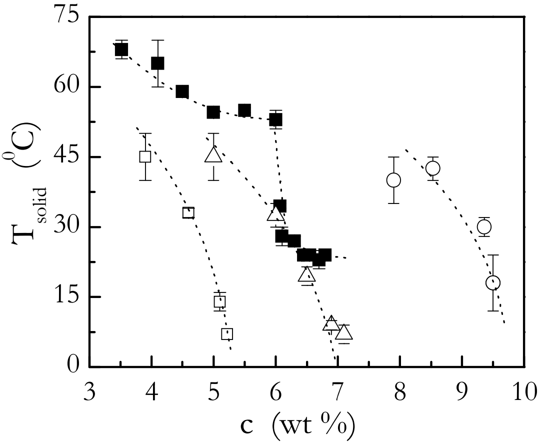

Figure 11: Vitrification temperature T_{solid} as function of polymer concentration c for stars in various solvents (□: 12880/decane, △: 12856/decane, O: 12828/decane, ■: 12880/tetradecane). Lines are drawn to guide the eye; they are state lines separating liquid (below) from glass. Data are taken from references [211, 225].

generic, at least for a wide class of soft materials that can increase their volume fraction at constant number concentration. Note that, for the core-corona star systems considered here, the size ratio of 'grafted' layer to central core is about 100 times larger than in most well-studied block copolymer micelles [141, 235-245] or tunable sterically stabilized colloids (see for example Ref. 81 and section 3.1 above].

With the rheological determination of the temperature for dynamic arrest (i.e, vitrification), T_{solid}, it is possible to construct kinetic state diagrams for different classes of ultrasoft colloids. Fig. 11 shows such a diagram, where it depicts T_{solid} as a function of the concentration for colloidal stars (with f = 128) in two different solvents, decane [212, 225] and tetradecane [211]. The dashed lines through the data represent state lines separating the liquid (below) from the dynamically arrested solid (above) regimes. The effects of solvent quality are evident and suggest that for the reduced solvent quality 12880/tetradecane system at the same star concentration, more thermal energy is needed to reach the vitrified state. Alternatively, a certain mass of star at a certain temperature can exhibit either liquid or solid response depending on the solvent used. Note that the extrapolated T_{solid} difference in the dilute limit ($c \rightarrow 0$) between the solvents reflects the difference in thermodynamic quality of the two solvents, as measured for example by the second virial coefficient or the hydrodynamic radius [211, 246]. A generic diagram can be obtained for different stars if an effective volume fraction is used instead of concentration [211].

A more rigorous description of this reversible thermal glass transition was obtained from the Molecular Dynamics (MD) simulations of Rissanou and Bitsanis with dense suspensions of the colloidal star polymers used in the experiments [229]. These star polymers were modeled as soft-spheres interacting via the theoretically developed potential of mean field; this potential allows for the temperature effect to be accounted for via the temperature-dependent hydrodynamic radius (Fig. 6a) and is given by Eq. (2) below [246, 229]:

$$\frac{U(r)}{k_B T} = \begin{cases} \infty & r < 2\alpha \\ U_o\left[-\ln y - \frac{9}{5}(1-y) + \frac{1}{3}(1-y^3) - \frac{1}{30}(1-y^6)\right] & 2\alpha < r < 2(a+L) \\ 0 & 2(a+L) < r \end{cases} \quad (2)$$

where $y = \dfrac{r-2a}{2L}$, $U_0 = \dfrac{\pi^2 L^3 f}{48 N l^2 a}$, $L \approx R_0 - a$.

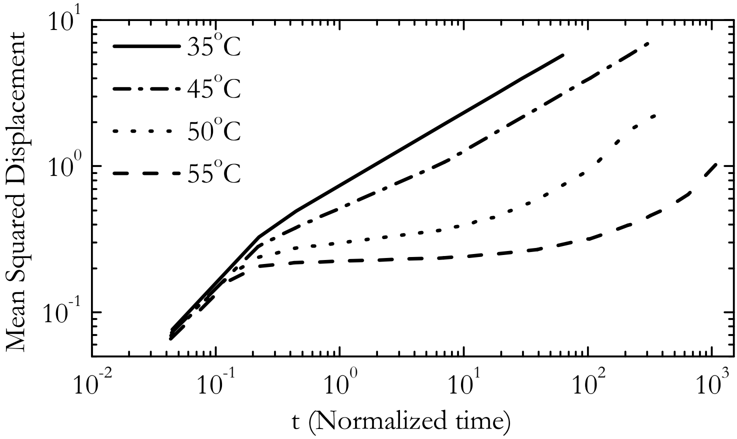

Figure 12: Star mean squared displacement as a function of time for temperatures between $T = 35\,^{\circ}\mathrm{C}$ and $T = 55\,^{\circ}\mathrm{C}$. Plateaux are evidence of "caging effects" at high temperatures. Data are taken from reference [229].

Results [229] indicate a transition towards a glassy state at a temperature very close to the one reported experimentally. The features of the transition are consistent with those of ideal glass transitions, as described by ideal Mode Coupling Theory [247, 248]. In particular, whereas typical liquid-like ordering (as reflected from the shape of the pair correlation function and the related structure factor) is manifested at the lowest temperature, at high temperatures a gradual split of the second peak of the structure factor is observed, along with the steady development of a 'shoulder' (incipient split) of the third peak and the flattening of the fourth peak; these are indications of the development of a crystalline (FCC) structure. Indeed, such microstructural changes reflect the competition between a 'frozen' crystalline state and a 'mobile' amorphous state. These new features are often suggestive of vitrification. Furthermore, the monitoring of the soft sphere mobility via the time dependence of the mean squared displacement (MSD) reveals important information (see Fig. 12): A linear time dependence, typical of Fickian diffusion, is very clear at 35°C (as well as below 35°C, not shown in the figure); a weak 'shoulder', indicative of a slight delay at intermediate times can be seen in the T=45°C curve. However, at 50°C and moreover at 55°C, the short range mobility is followed by a pronounced stagnation, which persists for two decades in the timescale of Fig. 12. Soft-sphere mobility recovers only at much longer times, and the resulting self diffusivity is substantially lower (by 2 orders of magnitude) than that observed in the liquid suspension (T $\leq$35 °C). This type of time evolution of the MSD curves is characteristic of "caging", i.e., the temporary confinement of particles in cages formed by their immediate neighbours [231-234] (see analogous studies with hard spheres [249, 4, 250]).

6.3. <u>Implications and relevence</u>

A number of interesting possibilities for the rational design and engineering of soft materials arise. Temperature is an advantageous volume fraction control parameter and can be used for monitoring the processing performance of a given formulation without the need for additives. To this end, the underlying challenge is the development of predictive tools for structures and transitions in colloidal systems of varying interactions, repulsive and attractive [251-253]. In addition, several complex structures are thermally responsive and yield inverse freezing [254, 255]; this is a potentially important feature for assemblies of biological relevance, such as hydrogels, [256-258]. Of course, such systems are characterized by a complex interplay of different interactions and the interpretation of their phenomenologically similar thermal freezing may be different; such is the case for systems exhibiting thermodynamic phase boundaries [106, 259]. We note in particular the work of Shay et al [106]. These authors investigated the thermoreversible gelation of polystyrene latex particles bearing grafted poly(ethylene oxide), PEO, chains of low molecular weight. In water, where PEO exhibits a LCST behaviour, as the temperature increased the frequency-dependent G' (reproduced here in Fig. 13) exhibited a remarkable resemblance with the star data of Fig. 5; of course, the explanation for the observed gelation in that case involved an attractive element due to the solvent conditions.

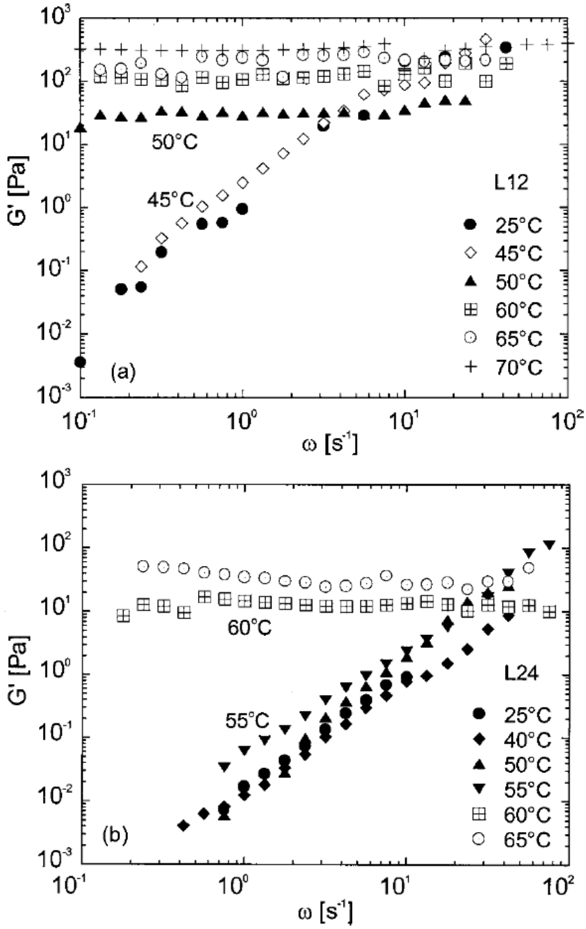

Figure 13 : Elastic modulus (G') as a function of frequency (ω) for dispersions at volume fraction φ=0.1 of two different PS latex colloids **(a)** the L12 latex with moderate PEO graft density and **(b)** the L24 latex with a high PEO graft density. Data are shown for a range of temperatures between 25 and 65°C. Adapted from reference [106].

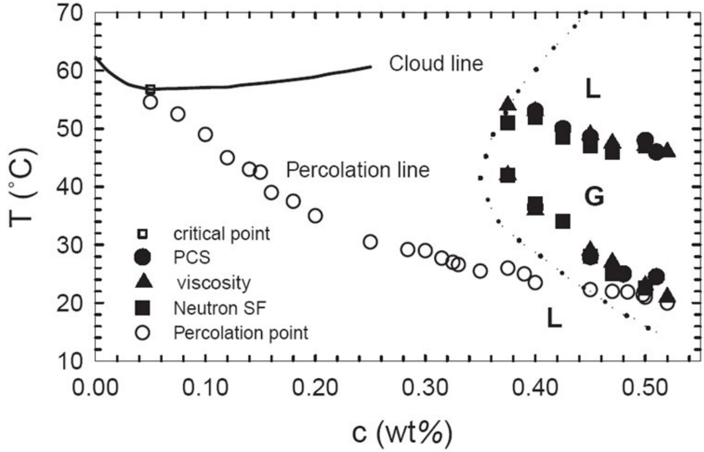

Figure 14: Phase diagram of the L64/D_2O pluronic system. The dotted line marks the equilibrium phase boundary between the disordered micellar phase (liquid) and the ordered, metastable, liquid crystal hexagonal phase. Solid symbols on the high-concentration side represent L(liquid)-G(glass)-L(liquid) transition boundaries. Note similarities of the percolation line and the Liquid-Glass line to the state lines of Fig. 11. Adapted from reference [260].

However, these data are suggestive of a universal thermal liquid-to-solid transition phenomenology, for systems with a range of soft interactions. Highly relevant is also the recent work of Mallamace and Chen [260-262]. They investigated in length aqueous solutions of a copolymer micellar system of the pluronic type using rheology and scattering. They reported a variety of equilibrium disordered and crystalline as well as metastable (gel and glassy) states, which were compiled in a proposed phase diagram of temperature against concentration. Parts of this diagram, which we present in Fig. 14, relating to the percolation and glass lines, exhibit a remarkable resemblance to the star state diagram of this work, and point to a universality of behaviour in these soft colloidal systems. On the other hand, it should be kept in mind that the pluronic micelles have attractive interactions, something presumably absent in the present star systems. Naturally, this phenomenon affects the self-assembly of soft matter and can be significant for the formation of novel supramolecular structures [263-265, 251-253].

As we note in Ref. [225], block copolymer micelles also exhibit this reversible thermal vitrification. Based, on the above discussion, the phenomenon should be universal. There is, however, an additional feature that merits attention. Sato et al [154] reported a similar thermoreversible effect, but upon cooling, for polystyrene-polyisoprene - polystyrene (SIS) and polystyrene - polyisoprene copolymers in an

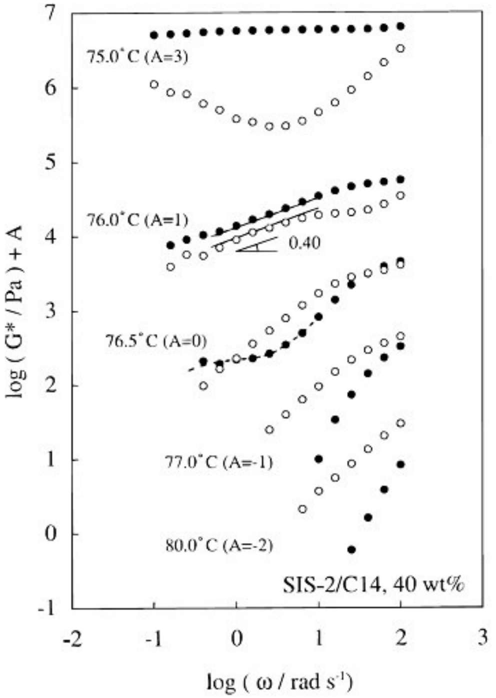

Figure 15: Storage and loss moduli, $G'(\omega)$ and $G''(\omega)$ (filled and unfilled symbols, respectively), of a 40 wt % SIS-2/tetradecane solution at various temperatures. The plots at each temperature are shifted vertically by the factor A as indicated for clarity. Adapted from reference [154].

isoprene-selective solvent, n-tetradecane. They assigned the liquid-to-solid transition with reducing temperature to gelation.

The change of linear viscoelastic spectra upon cooling through the transition is remarkable, and indeed the system goes through a critical gel-like transition [266], as seen in Fig. 15 which we include for illustration purposes. Another way to interpret the data of this figure is to consider the liquid-to-solid transition as the volume fraction of the micelles changes (through the change of temperature). In such a case, the rheological signature of the lowest temperature is that of a colloidal glass [267, see also Fig. 16], and the system undergoes a rather gradual transition from liquid to glass, through a critical gel-like regime; this, in fact can be also observed by a closer inspection at the hard-sphere glass data of [267] in Fig. 16. Moreover, a similar

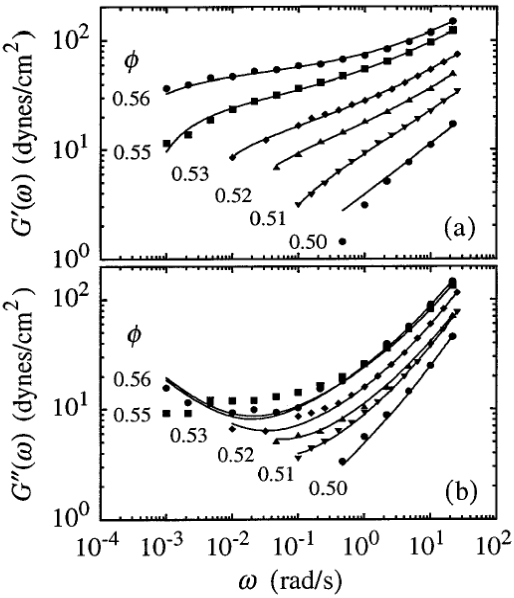

Figure 16: The frequency dependences of the storage **(a)** and loss **(b)** moduli for different volume fractions, φ, of PMMA-HSA hard spheres. The solid lines represent MCT predictions (not further discussed here). Adapted from reference [267].

gradual liquid-to-glass rheological transition through a gel-like state was also reported for colloidal stars in good solvent by varying the volume fraction [268] and can be also observed in the data of Chen and Mallamace for pluoronic micelles [262], as well as those of Bhatia and Mourchid for block polyelectrolyte micelles [269]. In the latter two cases, attractive glasses were formed. This brings up issue of analogies between gel and glass transtions [270, 271, 231] and may have consequences in the rheology of concentrated suspensions [272, 273, 216], and therefore needs further work in the future.

Lastly, a remark on the analogy to thermodynamic transitions is in order. The concept of inverse melting was reported for different semi-crystalline polymers [274, 275]; in particular, a heating-induced crystallization and a re-entrant melting upon further increase of the temperature were reported. Although this phenomenon, which goes back to the re-entrant phase diagram proposed by Tammann [276] has a completely different origin (large difference in specific volume between liquid and crystal phases) than the present heating-induced vitrification of the model soft colloids, the analogies of behaviour are intriguing and the role of entropy is of great significance. For completion, we mention that preliminary rheological measurements with the concentrated star suspensions which form glassy states upon heating as already discussed, are suggestive of a tendency for melting upon further increase of temperature [277].

7. DEPLETION IN GLASSY STAR-LINEAR POLYMER MIXTURES

7.1. <u>The phenomenon</u>

It is well known that when non-adsorbing polymers (of size R_g) are added to stable colloidal suspensions, the particles (of size $R>>R_g$) experience an induced depletion attraction, whose origin is the unbalanced osmotic pressure due to the exclusion of the polymer molecules from the region between colloids [11]. The key parameters controlling the effect are the size ratio $\xi=R/R_g$ (controls the range of the attraction) and the polymer concentration (controls the strength of the attraction).

The essential physics was first proposed by Asakura and Oosawa [278, 279] and later by Vrij [280]. The classic works on the experimental and theoretical phase behavior of a colloid-polymer mixture are those of Russel and co-workers [281-283] and Lekkerkerker et al. [284]. It was found that when ξ was less than a certain critical value ξ_c (~0.33 [285]), the addition of polymer basically expanded the fluid-crystal coexistence region of pure hard spheres (the latter occurring at a colloid volume fraction between 0.494 and 0.545); on the other hand, for $\xi>\xi_c$ a colloidal liquid was obtained, exhibiting a colloidal gas-liquid critical point and a region of three-phase coexistence (colloidal gas, liquid and crystal). The implications to the rheology and microstructure of suspensions are significant [11, 286-288]. A summary of the key findings can be found in [11, 289, 290].

An interesting extension of this work is exploring the non-ideality of the depletant. To this end, mixtures of colloids and star polymers (with functionalities up to 32) were studied [291-293]. The results indicate that the observed phase diagrams exhibit many similarities with the colloid-linear polymer mixtures and further suggest that stars with f=32 behave like hard spheres, provided that they are smaller than the hard particles.

With this background, it is tempting to consider mixtures of colloidal stars and linear chains, the latter now serving as depletants. Indeed, this is what we shall describe below. Given the difficulty in observing crystalline phase in stars, we focused on the high star volume fraction regime, i.e., the frozen state.

Experimental evidence from rheology and scattering suggests that, when a linear polymer is added to a glassy colloidal star suspension, it can induce melting depending on its relative size with respect to the star and/or concentration; within the melted region, the reduced star viscosity drops upon further addition of linear polymer [294]. This is a direct consequence of the depletion effect induced by the linear polymer additive, and can be explained in terms of the effective star-star interaction in the presence of linear polymer [42, 294, 11, 46]. Dynamic rheology is shown to be a

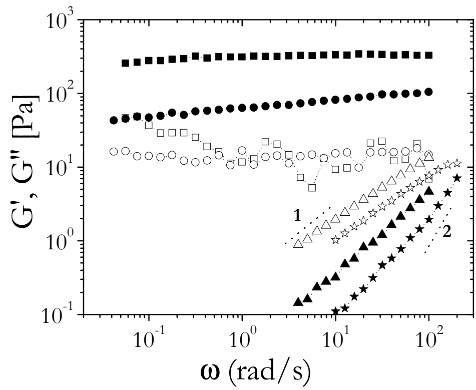

Figure 17: Dynamic frequency sweeps of LS6/toluene 2.5 wt% solution (■,□) at 10°C and several mixtures with linear polymer of molecular mass 22600 g/mol and different concentrations, C_{lin}: (●,○) 0.6 wt%, (▲,△) 1.53 wt%, (filled star , open star) 2.51 wt% (Solid symbols: G'; Open symbols: G'').

powerful tool for probing this type of solid-to-liquid transition. A characteristic example is shown in Fig. 17 for a vitrified colloidal star suspension of LS6 (see Table 1) at a concentration of 2.5 wt% in the athermal solvent toluene, which exhibits nearly frequency-independent G' and G'' (with $G'' < G'$), over a wide frequency range. It is important to note here, that the rheological signature of the star glass is identical to that of glasses from hard spheres [267] or other soft colloids [see for example 105, 260, 262]. To illustrate this point, we show here (Fig. 16), for comparison, a classic set of data from the literature, on concentrated PMMA-HSA suspensions approaching the glass transition [267].

Furthermore, Helgeson et al [61] showed recently that the star glass data can be described with the modified mode coupling theory methodology, exactly as in the case of hard spheres of Fig. 16 (note that qualitatively the same viscoelastic spectrum signifies the response of concentrated microgel solutions as well, see references 295 and 296). The addition of linear homopolymer chains (1,4-polybutadiene) with molecular mass of 22600 g/mol in Fig. 17 to the star glass, at different concentrations (here, from 0.6 wt% to 2.51 wt%), leads to a reduction of the G' as the concentration is increased, and eventually to terminal flow $(G'' < G', G' \sim \omega^2, G'' \sim \omega)$. The same qualitative effect (melting) is achieved if the linear polymer is added at constant concentration but increasing molecular mass.

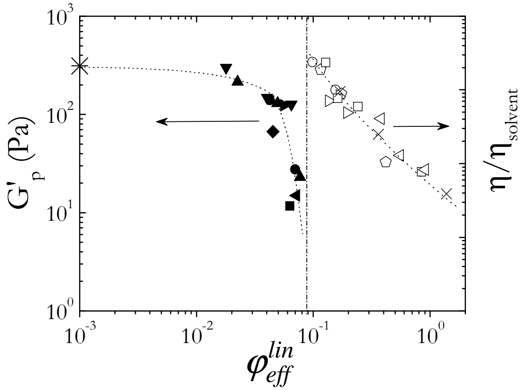

Figure 18: Plateau moduli $G_p^{'}$ of the glasses (solid symbols) and reduced zero-shear viscosities $\eta/\eta_{solvent}$ of the liquids (open symbols) for various star-linear polymer mixtures at constant star concentration 2.5 wt % in toluene and different linear polymer concentration and/or molecular mass in g/mol (*:LS6, ▼:LS6/1000, ▲:LS6/2730, ●: LS6/6250, ▶: LS6/9150, ◆: LS6/22600, ■: LS6/61000, X: LS6/105700, ◀: LS6/165000) against the effective volume fraction (reduced concentration) of the linear polymer, φ_{eff}^{lin}. Data taken from reference [294].

One way to combine the molecular weight and concentration influences is to plot both the storage (or plateau) moduli of the various solid-like star-linear polymer mixtures and the reduced (to the solvent) zero-shear viscosities of the depletion-melted mixtures for all linear polymer concentrations and molecular masses. As seen in Fig. 18, all data collapse into master curves when plotted against the reduced linear polymer concentration c_{lin} / c_{lin}^{*} (i.e., the effective linear homopolymer volume fraction φ_{eff}^{lin}) [294]. This type of kinetic transition can be represented in the state diagram of Fig. 19, in terms of linear polymer concentration against linear polymer molecular mass for a fixed concentration of the colloidal star suspension. Starting from a vitrified star suspension, the state diagram of the mixture shows areas of solid and liquid states, depending on the concentration and molecular mass of the added linear polymer. Interestingly, as the molecular mass of the added polymer increases beyond a threshold (of about 300,000 g/mol here), a re-entrant glassy-like state is probed (see the lighr-gray grid area of Fig. 19).

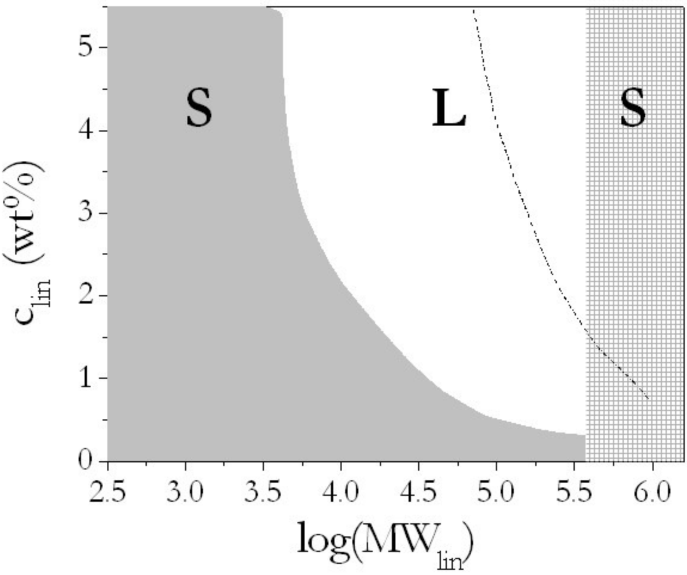

Figure 19: Rheological state diagram of star-linear polymer mixtures in toluene, in terms of concentration of the added linear polymer against the respective molecular mass. Star concentration is 2.5 wt% (in the glassy state). Light and dark gray regions denote solid-like behaviour (S) and white denotes the liquid-like behaviour (L). The dashed line marks the linear chain overlap concentrations c^*_{lin}. For $MW_{lin} < 100000$ g/mol, c^*_{lin} lies above 6 wt% (not seen in the figure). The light-gray grid region on the right denotes the re-entrant solid (glassy) state.

The linear viscoelastic response in this region is qualitatively different from the low-molecular mass glass, with a power-law G' and additional relaxations (seen clearly in G''); this can be seen in the comparative plot of Fig. 20. Note also that G' of the re-entrant glass drops faster as the frequency is lowered.

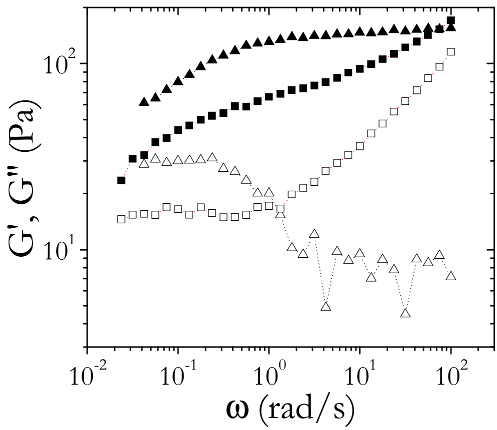

Figure 20: Dynamic frequency sweeps of mixtures LS6/linear polymer in toluene with star and linear concentration 2.5 wt% and 1.53 wt%, respectively, for different linear polymer molecular masses: (▲,△) 6250 g/mol (glass) and (■,□) 1243000 g/mol (re-entrant glass). (Solid symbols: G' ; Open symbols: G'').

7.2. Interpretation

The polymer-mediated melting phenomenon was accounted for Likos, who used the effective interactions between the components of the mixture [42, 294, 297]. It was demonstrated that the addition of the chains causes a drastic decrease of the peak of the star-star structure factor, with the effect becoming stronger as the chain size (or concentration) increased; this conforms to the melting picture. A typical theoretical prediction is depicted in Fig. 21a, where the stars here are considered to crystallize. Whereas this was not the case experimentally, the analogy holds here: melting of the structure (loss of correlations). Indeed, in Fig. 21b we show SANS data with selected mixtures, which confirm the predictions [294]. It appears that the linear chains tend to occupy spaces in the interstitial area between overlapping stars, and thus reduce the fluctuations in the system.

These results can be understood in terms of an effective potential $U_{eff}(r)$ acting between the stars in the presence of the linear chains, related to the star-star radial distribution function. This was calculated by Likos [294, 297] and is depicted in

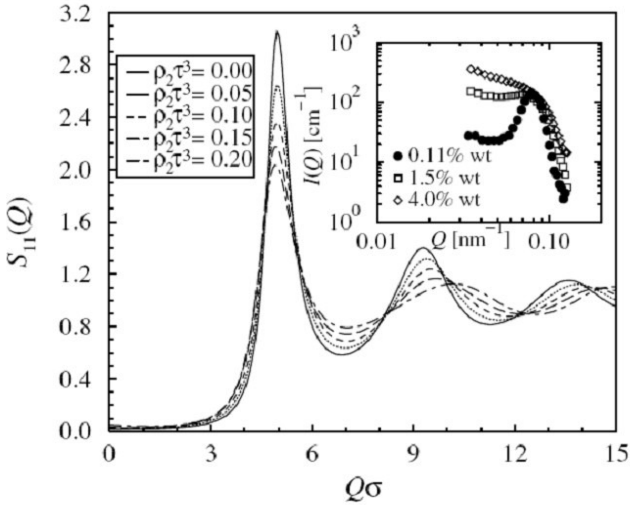

Figure 21: The calculated structure factor $S_{11}(Q)$ of the stars (component 1) at a normalized star density 0.35, for various normalized concentrations of added linear polymer chains and for size ratio q =0.30; and **(inset)** star-star SANS scattering intensities from a star-linear polymer mixture at the same size ratio, at a star concentration c_{star}=2.5 wt% and for different linear chain concentrations (c_{lin}: ●: 0.11 wt%, □: 1.5 wt%, ◇: 4 wt%). Shown is only the Q range around the first maximum of I(Q). Data taken from reference [294].

Fig. 22. In fact, the linear chains reduce the range of the bare star-star repulsion due to the osmotic force they exert on the stars, which is manifested as a depletion mechanism. Indeed, smaller chains cause an effective attraction between larger colloidal particles [42, 297-305]. In the case at hand, the depletion attraction is superimposed on the soft repulsion among the stars, and thus its dominant effect is to bring about a reduced repulsion among them. As the interstar repulsions become weaker, the correlations in the fluid are reduced and the latter regains stability. The further experimental confirmation of the depletion mechanism comes from the hydronamic radii measured with DLS in dilute star suspensions as function of the added linear homopolymer concentration, depicted in the inset of Fig. 22. Note that at high c_{lin}/c_{lin}^* the effective attraction dominates, yielding cluster formation [297].

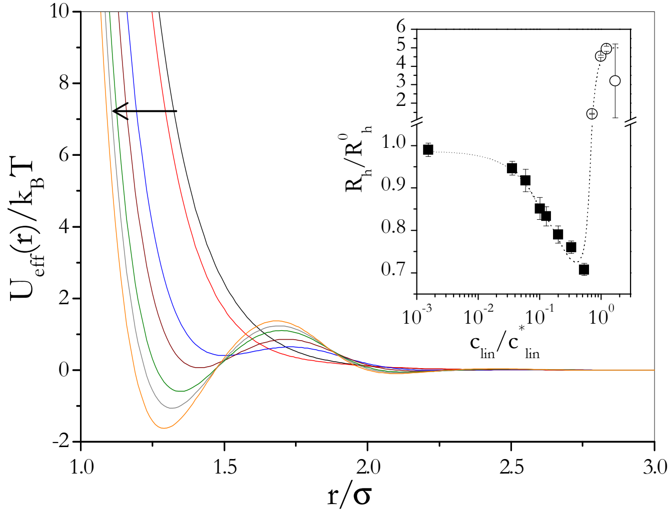

Figure 22: The effective star-star potential $U_{eff}(r)/k_BT$, mediated by polymer chains of size ratio q=0.44, at various linear polymer volume fractions c/c^*_{lin} from right to left, as shown by the arrow (0.00, 0.104, 0.418, 0.522, 0.626, 0.679, 0.731). Inset: Normalized effective hydrodynamic radius of the star R_h/R_h^0 as a function of c_{lin}/c^*_{lin}. The dotted line is drawn to guide the eye. Open symbols correspond to the star cluster (see text). Data taken from reference [297].

The cartoon of Fig. 23 attempts to capture the main physical difference between small and large linear chains when interacting with a single star. The idea is that in the latter case the large chains (with respect to the star arm) create an osmotic force that shrinks the star and eventually yields star-star clustering at high concentrations (see also Fig. 22), analogous to the well-known manifestation of depletion in hard sphere/linear polymer mixtures [11, 288-291]; these clusters appear to be stable [302, 305, 306]. This latter indication should be assessed in view of recent suggestions based on colloid-polymer depletion gels, according to which dynamic arrest appears to occur via cluster growth and association [307]. On the macroscopic level, the depletion relates to reduced correlations, enhanced mobility and a fluid response [294, 301].

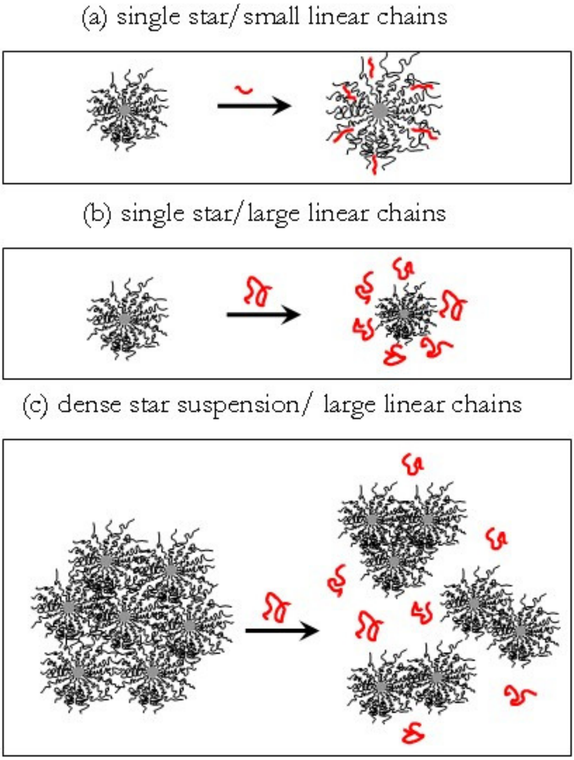

Figure 23: Cartoon illustration of the polymer-mediated melting phenomenon. Small linear chains can swell a single star (a), whereas large chains will shrink it (b). In dense suspension, the osmotic forces of the large linear chains lead to depletion (c), as discussed in the text.

Naturally, the type of depletion discussed here (i.e., with effective pair potentials) takes place when the size of the linear polymer (typically, its hydrodynamic radius, R_h^{lin}) is smaller than that of the star (R_h^{star}) [11, 289, 294, 305, 293-298], i.e., in the colloid limit. In fact, for values of the size ratio $S = R_h^{star} / R_h^{lin} > 2$ this depletion mechanism is active and enhanced when S decreases, but it breaks down around $S \sim 0(1)$ [294]. In the range S<1, i.e., the so-called protein limit, the behavior of a colloid-polymer mixture is changing, and many-body effects need being considered [308-310].

In the present star/linear polymer mixture, the experimental phenomenology (Fig. 19, 20) suggests a re-entrant solid-like behavior that is reminiscent of the bridging flocculation reported in the colloid-polymer literacture [311, 11]. It should be noted however, that the latter effect is usually a consequence of adsorption of the polymer onto colloidal particles, something that is not the case in the mixtures considered here. On the other hand, the possible interaction of star arms with linear chains (due to the star structure, as illustrated in Fig. 3), makes this analogy relevant for further consideration. A recent detailed study of the depletion mechanism effects of linear chains in star-linear polymer mixtures [306] considered size ratios in the range $2<S<10$; although smaller ratios were not studied, in that range the linear polymer-mediated binary star effective interaction was found to be insensitive to the linear polymer concentration. This was in agreement with the experimental data [301, 294] and tentatively attributed to the worsening of the solvent quality for the stars as linear chains are added; beyond a threshold (overlap concentration), the theta state is reached [306].

These intriguing findings can be compared against those from more conventional colloid/polymer mixtures. In these systems, addition of small amount of polymer indeed leads to the melting of the colloidal glass; however, upon increase of the polymer concentration a new attractive glass emerges [59, 87, 299, 305, 312, 313], and this phenomenon is restricted to small polymer-to-colloid size ratios. Therefore, a universal picture of glassy states and their manipulation and transitions seems to emerge. Evidently, this also sets the stage for further work that is necessary in this direction.

7.3. Implications and relevance

A key point to address, again, is the rheological behavior of the star glass. As already mentioned, it is qualitatively identical to hard colloidal glasses. In addition, other liquid-to-solid transitions of colloidal particles of varying interactions, such as flocculation, exhibit the same phenomenology [91, 260-282, 314]; this brings up again the issue of distinguishing glasses from gels [231, 305], which however is not the subject of this work. The star systems here are considered to be in the glassy state on the account of their high volume fraction and repulsive pair interactions. The polymer-induced melting of the soft colloidal solid brings to mind analogies to the observed melting of a glass formed in a binary mixture of hard sphere-like microgel particles upon addition of chains [299, 312, 315], among other examples mentioned above. In fact, the proposed kinetic phase diagram for the microgel case (which we reproduce here for illustration purposes in Fig. 24) is very similar to that of Fig.19 for the present star/linear polymer mixtures. As that effect has been attributed to chain-mediated attractions between the microgels, it has been qualitatively modeled by a square-well potential acting between the spheres [60, 300, 316, 317].

Of particular interest is the distinction of glass from liquid behavior on the grounds of a different response of the intermediate scattering functions, i.e., non-ergodic and ergodic, respectively. This is exactly the case for the star/linear polymer system [297]; moreover, in the latter case the non-ergodic behavior was directly correlated with a solid-like rheological response, both signatures being characteristic features of colloidal glasses [268]. The connection between the two reported

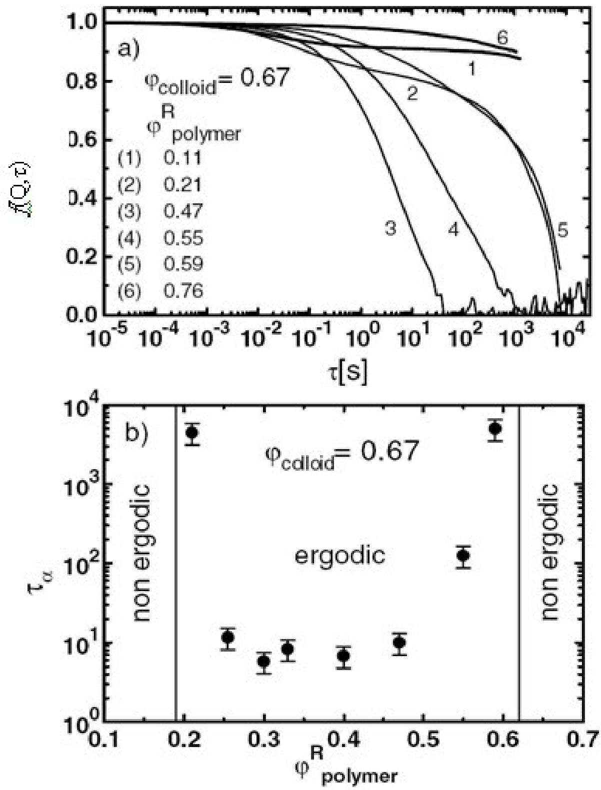

Figure 24: Effect of increasing the free polymer volume fraction $\varphi^R_{polymer}$ on the dynamics of a colloidal microgel suspension in a glassy state close to random close packing ($\varphi_{colloid} = 0.67$) indicating the phenomenon of re-entrant melting. (a) Density autocorrelation functions *f*(Q,τ) (probed by DLS at a scattering vector corresponding to the peak maximum of S(Q) of the pure colloid suspension at its glass-transition volume fraction $\varphi_g \approx 0.595$). The polymer reservoir volume fractions $\varphi^R_{polymer}$ are indicated by the numbers at the curves. Lines 1 and 6 correspond to nonergodic (glassy) samples. (b) Structural relaxation times τ_α versus polymer reservoir volume fraction $\varphi^R_{polymer}$ polymer. The vertical lines schematically indicate the transition lines to the respective nonergodic states. Adapted from reference [312].

phenomena suggests a universality of the effect of added polymers in mediating the melting of soft solids, with profound implications in their flow control .

Another intriguing connection is that of the present glass melting phenomenon with the suppression of crystallization induced by the depletant concentration [317-319]. This, again points to a potential universality of the effects of depletion forces in causing eventually melting of solid structures.

8. DEPLETION IN GLASSY BINARY ASYMMETRIC STAR MIXTURES

8.1. The phenomenon and its interpretation

One of the challenges emerging from the depletion studies discussed in the previous section, is exploring the role of the depletant. In particular, an interesting question is what would happen if the ideal linear polymer chain additive is replaced by a (small) star polymer additive; this yields a binary asymmetric star mixture. The controlling parameters are the same, i.e, the size ratio of small-to-large star, ξ, and the concentration of the added small (depletant) star, here in normalized units $\rho_2\sigma_1^3$ (added small star being denoted as component 2). Small amplitude oscillatory shear measurements performed with such mixtures, where the large colloidal stars were in the glassy state and the small stars (of lower functionality and/or arm molecular weight) were added at different concentrations, revealed qualitative similarities to the star-linear polymer case, but still a more complex, behaviour: a melting of the glass upon addition of the small stars. However, with increasing the star size ratio ξ, a re-entrant glass was observed [320-322]. Typical results are depicted in Fig. 25. It is clear that at low concentration of the small star the mixture exhibits the typical solid-like behaviour, observed in colloidal glasses [61, 267, 323, 296]; this is termed "single glass" in the sense that only the large star is vitrified, whereas the small is able to move (this was deduced from MCT calculations [247, 35, 320, 321, 324, 325]). As we add more of the small star of constant functionality and molecular mass (Table 1), the glass gradually weakens, as reflected in the rheological signal. In fact, the mixture's plateau modulus (high-frequency G' limit) decreases, at the same time, the G'' remains virtually unchanged, suggesting that the key effect of the additive is the softening of the cage elasticity of the big stars. Eventually, as the small star's concentration increases further, the cage apparently opens up, the glass melts, and the classic viscoelastic liquid response is reached. This is a remarkable finding given the change of viscoelastic moduli by orders of magnitude upon changing the concentration of the small star (here, basically doubling the concentration). Note that the same behaviour is observed qualitatively, when we keep the concentration of the added small star constant while we change its molecular mass [320, 321].

Similarly to the star/linear polymer mixtures of the previous section, this rheological information can be compiled into a kinetic state diagram of concentration of the added small star against its molecular mass, for constant concentration of the large star. In this diagram, shown in Fig. 26a, where we map the rheological signature of the star mixture as we change the additive. One can observe that by increasing the

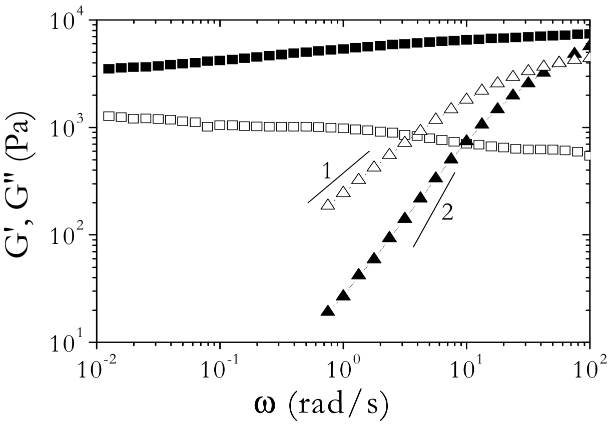

Figure 25: Dynamic frequency sweeps of binary asymmetric star mixtures LS4/6430 in toluene with constant LS4 concentration 2.5 wt% (in the glassy state) but different concentrations of 6430 [■,□: 0.5 wt%, ▲,△: 3.5 wt%] (Solid symbols: G' ; Open symbols: G'').

concentration of a given small star, the mixture is transformed from a solid (glass) to a viscoelastic liquid. On the other hand, at constant concentration of the small star, increasing its molecular mass yields a melting of the glass; eventually, at very high molecular mass, there is an apparent tendency for a re-entrant vitrification of the mixture, and the overall kinetic phase diagram takes a U-shape. Moreover, for each combination of big glassy star and functionality of small added star there is one U-shape curve signifying the liquid-to-glass boundary. These pertinent findings are qualitatively similar to the predicted state diagrams obtained from MCT (Fig.26b) [320, 321]. All related theoretical analysis and MCT calculations disussed in this context were carried out by Likos, Mayer, Zaccarelli and co-workers [320,321]. It should be noted here, that the apparent number of experimental data points is a consequence of the limited availability of model star polymers. On the other hand, for each size ratio several experiments were performed with varying the concentrattion of the small star additive. The data points indicated on the U-shape kinetic diagrams of Fig. 26 mark the higher concentration of added small star where glass-like behaviour was detected, and respectively, the lower additive concentration where liquid-like behavior was detected for a particular star/star polymer mixture.

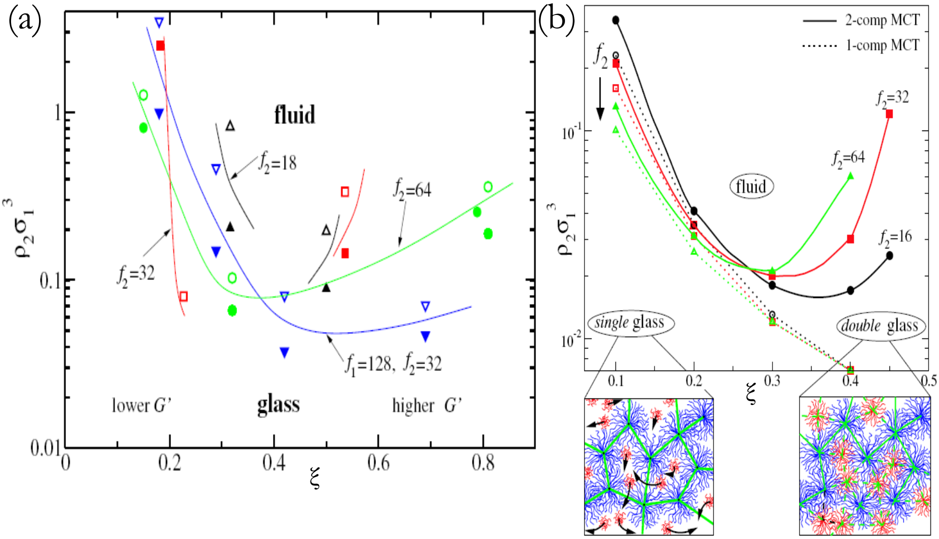

Figure 26: (a) Experimental kinetic phase diagram of binary star mixtures, indicating regions of liquid and glass for different concentrations of added small star $\rho_2\sigma_1^3$ and size ratios ξ. Large stars of functionalities f_1=270 and 128 were used, with normalized concentrations $\rho_1\sigma_1^3$=0.345 and 0.412, respectively. Open symbols denote a liquid and solid symbols a solid (glass) state. Only the data points closest to the melting lines are shown here. The lines through the data, passing above the full symbols and below the empty ones, are guides to the eye.

(b) Respective theoretical kinetic phase diagram of binary star mixtures, calculated using MCT. The large-star functionality and concentration are fixed at the values f_1=270 and $\rho_1\sigma_1^3$=0.345. The diagram is shown for three different functionalities f_2 of the small stars. Circles: f_2 =16; squares: f_2=32; triangles: f_2 =64. The solid lines going through the calculated points are guides to the eye. The dotted lines and respective data reperecent MCT without considering double glass scenario (see ref. 320). The cartoons display local arrangements in a single big-star glass with mobile small stars (left) and in a double glass in which there is mutual caging of both components (right). Single glass has lower elasic moduli than the double glass. Data taken from reference [320].

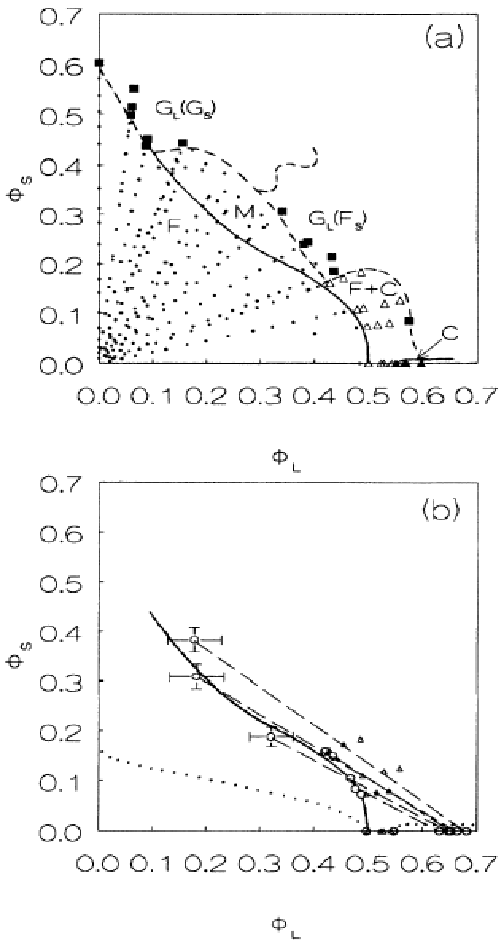

Figure 27: **(a)** Phase diagram of the binary hard sphere mixture. Dots represent homogeneous fluids, open triangles are samples separating into fluid (F) and crystal (C), filled triangles are completely crystalline, filled squares are glassy samples (G). The solid line is the fluid-solid binodal, dashed lines are glass transition lines.

(b) Construction of the fluid-solid binodal (solid line). Triangles are compositions separating into fluid and crystal. Dashed lines are tie lines connecting coexisting compositions (circles). The dotted line is the theoretical prediction. Adapted from reference [326].

Again, as in the case of star-linear polymer mixtures, we note here that for large values of ξ, this simple depletion scenario does not hold anymore (see also relevant discussion in Section 7); in fact, the theoretical analysis is restricted to $0.1 \leq \xi \leq 0.45$, and beyond the upper threshold no melting is predicted. A simple explanation suggests that, as ξ increases, the small stars become as large as the voids in the glassy matrix of the large stars, and get trapped there, forming themselves a glass within the big star glass: this is the so called double glass (see cartoon in Fig. 26b). In such a case, the small stars contribute to the cage formation. Naturally, as ξ grows, this trapping mechanism becomes more effective and the slope of the vitrification line is reversed; this is described by the two-component MCT [320, 321]. As ξ grows further, the caging mechanism becomes so strong, that no melting is predicted. Therefore, the important result of this analysis is the prediction of two different glassy states under the melting boundary: a single glass (at lower ξ), when the small star component remains mobile, and a double glass (at higher ξ), when both star components become arrested (cartoon of Fig. 26b). Note that the same type of behavior was reported for binary mixtures of hard sphere colloids with large size asymmetry [326], with the important distinction that in that case a melting of the large hard sphere glass upon addition of the small component was not observed. In Fig. 27, we reproduce the phase diagram of the binary hard sphere mixture [326] for comparison.

The two different glasses have distinct signatures: as seen in Fig. 28 (a) and (b), the non-ergodicity factors are different. In fact, it appears that the double glass is strongly non-ergodic in the sense that both components exhibit non-ergodic response. On the other hand, the single glass is weakly non-ergodic, as only the large star component exhibits a non-ergodic response. In addition, the elastic modulus of the former is clearly larger, and this has been confirmed experimentally as well; actually, the dependence of the experimental and predicted normalized G' on ξ is depicted in Fig. 28 (c). In the single glass, the fluid-like small star component does not contribute to G' and it contributes to the softening of the cages formed by the large star component; this leads to a lower G'. On the other hand, as ξ increases, the small stars participate to the glass formation themselves, and thus they contribute to the enhancement of the G'. The experimental support of this trend provides a confirmation of the single/double glass picture put forward. Note that different types of glasses have been observed experimentally in PMMA/PS colloid/polymer mixtures [327], pluronic copolymer micelles [328, 261, 262], micellar solutions of associative polystyrene-poly(acrylic acid) block copolymers [329, 330], and in thermally reversible coated silica suspensions [331]. Whereas a distinct difference in the moduli and non-ergodicity parameter between glasses was detected, all cases involved repulsive-to-attractive glass transitions. Here it appears that as the strength of depletion increases in the single-glass and the double-glass states, re-entrant attractive and repulsive glasses are formed respectively [332, 333]. Nevertheless, a universal picture may emerge, suggesting ways to tune the properties of disordered colloidal systems to obtain different glassy states, and thus different rheological properties [332-334, 23, 253]

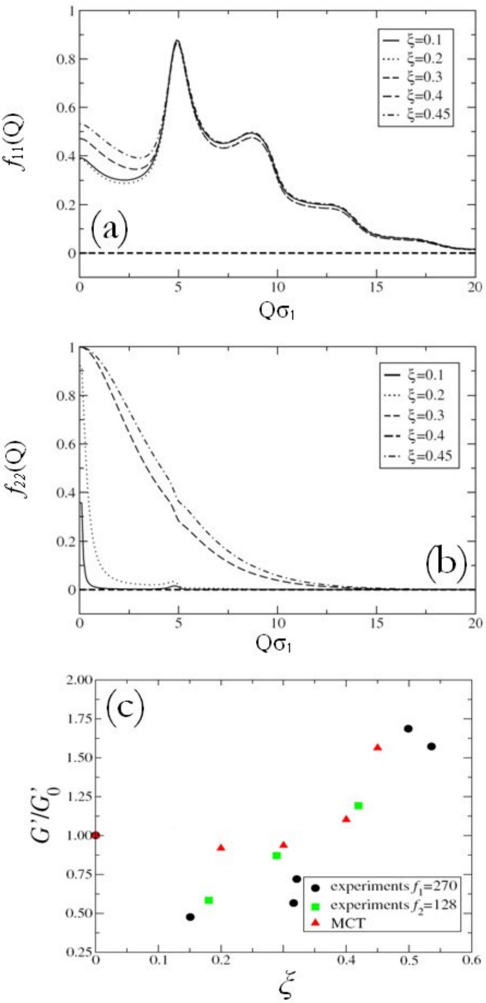

Figure 28: The nonergodicity factors $f_{11}(k)$ (**a**) and $f_{22}(k)$ (**b**) of the large and small star components, respectively, for f_1=270, f_2=32, $\rho_2\sigma_1^3$=0.02, at different ξ values. Note that for ξ = 0.3, the system is ergodic. **(c)** Plot of the ratio G'/G'_0, where G'_0 is the modulus of the big star system without additive, against the size ratio ξ close to melting. Theory refers to the case f_2=32, while experiments refer to a compilation of several measured elastic moduli of star-star mixtures, obtained with different big and small stars at various concentrations of the additives. Data taken from reference [320].

9. THERMAL VITRIFICATION IN STAR MIXTURES

9.1. Relevance

We revisit the problem of heating-induced glass transition of the colloidal stars (discussed in section 6) and consider a star/linear polymer mixture, where the linear chains interact with the stars, as discussed in section 7; depending on their size ratio, they may swell the stars or deplete them [211, 297]. This situation can, in fact, be realized by replacing the athermal solvent of the star-based mixtures in sections 7 and 8 above, with a solvent of intermediate quality. Indeed, Fig. 29 depicts dynamic frequency sweeps of the star/linear mixture 12880/1000 (1000 g/mol is the molecular mass of the linear polymer; concentration was c_{lin}=1.4 wt%) [301] in decane, at constant star concentration (c_{12880}=3.9 wt%) and different temperatures. It is observed that at low temperatures the system is liquid and from 7 to 10°C there is virtually no change in its rheological behavior. Then, at 15°C the sample still exhibits a liquid-like response, but with a slight enhancement of the loss modulus and a weaker increase of

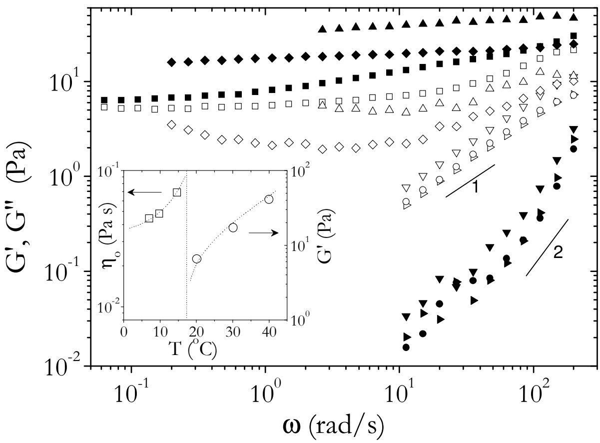

Figure 29: Dynamic frequency sweeps of G' (closed symbols) and G'' (open symbols) for 3.9 wt% 12880 in the mixture decane/linear 1,4-polybutadiene 1000 g/mol, (linear polymer concentration was c_{lin}=1.4 wt%), at different temperatures: 7°C (▷), 10°C (●), 15°C (▼), 20°C (■), 30°C (◆), and 40°C (▲). Inset: For the same system, the temperature evolution of zero-shear viscosity (□) in the liquid regime and plateau modulus (○) in the solid regime are shown . The vertical line indicates the vitrification temperature. The dotted lines are drawn to guide the eye. Data taken from reference [301].

the elastic modulus. At 20°C however, the sample solidifies and exhibits the rheological signature of a reversible weak soft glass [61, 323]. Further increase of temperature (up to 40°C here) yields a stronger caging effect [320, 321], thus glass, as judged by the increase of G'.

The temperature dependence of the zero shear viscosity (η_o) of the liquid and plateau modulus of the glass (G'), are depicted in the inset of Fig. 29, and bring analogies to the plot of Fig. 18 as a means for determining the glass transition Whereas in the latter case the glass transition volume fraction is determined, in the present case the effective colloidal glass transition temperature is obtained. To rationalize this behaviour, which is qualitatively similar to that discussed in section 6, it is instructive to probe the change of hydrodynamic radius of the star suspended in the linear polymer solution, as function of temperature (Fig. 30). Clearly, the increase of volume fraction is again responsible for the kinetic freezing of the mixture. In this case, however, a more complex freezing process takes place, because of the presence of the linear chains. The latter in the present case are small enough to penetrate the stars (Fig. 23a) and induce an additional swelling effect, whose consequences are evident in the vitrification process, discussed in terms of state boundaries below.

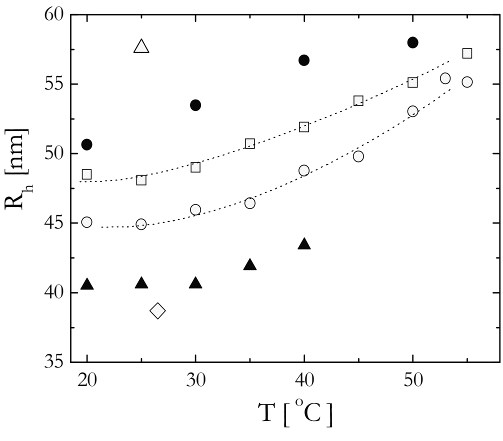

Figure 30: Temperature dependence of the hydrodynamic radius, R_h, of 12880 star in solutions of linear 1,4-polybutadienes in decane at different molecular masses: 1000 g/mol (●) and 165 000 g/mol (▲). The star concentrations are 0.015 and 0.010 wt %, whereas the linear polymer concentrations are 1.4 and 1.1 wt %, respectively. Also shown in this plot are the R_h (T) data for 12880 in net decane (□) and tetradecane (○), as well as the limiting values for athermal solvent cyclohexane (△, measured at 25 °C), and theta-solvent dioxane (◇, measured at 26.5 °C). Data taken from reference [211, 301].

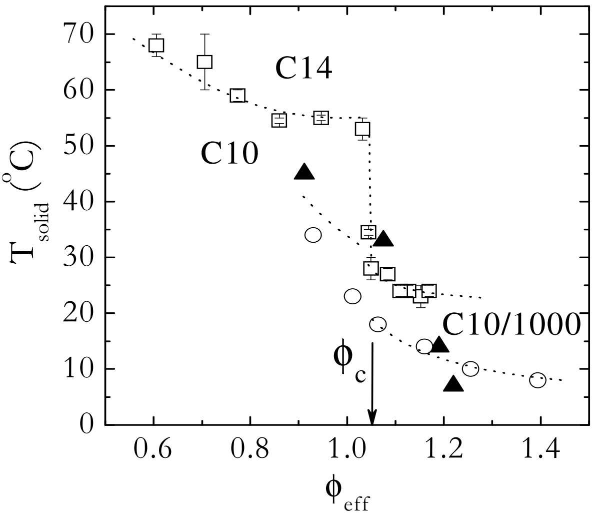

Figure 31: Vitrification temperature T_{solid} as function of the effective volume fraction φ_{eff} for 12880 in three solvents: decane (C10, ▲); tetradecane (C14, □); decane/short linear chains (C10/1000, ○). Lines are drawn to guide the eye. The vertical arrow indicates the critical volume fraction φ_c (see text). Data taken from reference [211, 301].

As in the case of the single star suspensions, the dynamic frequency sweeps at different temperatures and dynamic temperature ramp experiments at different frequencies can be compiled into a jamming state diagram, which is depicted in Fig. 31. There, the T_{solid} of different 12880/1000 mixtures in decane (with a linear-to-star size ratio of about 0.04) for different effective volume fractions of 12880 is shown, with a constant linear polymer concentration c_{lin}=1.4 wt% (thus the solvent C10/1000 exactly the same for all star solutions considered) [301]. For comparison, this figure includes also the T_{solid} data for 12880 in neat decane [212, 225] and tetradecane [211]. The data strongly indicate that the addition of the small linear chains reduces the T_{solid}. This reduction is smaller as c_{12880} increases but this may relate to the fact that eventually at high c_{12880} the T_{solid} should be independent of c_{12880} (as it has been observed for 12880 in tetradecane) [211]. This result is a manifestation of the effective improvement of solvent quality upon addition of small linear chains which can penetrate the stars, and consequently swell them. Eventually as the temperature increases in this particular example, the hard sphere limit is virtually reached at T=50ºC. In fact, if we consider the concentration of c_{12880}=4.5 wt% in Fig. 31, the effect of solvent quality on T_{solid} is remarkable: the highest T_{solid} is exhibited by the poorest solvent, tetradecane (the 4.5 wt% corresponds to effective volume fraction $\varphi_{eff} \sim 0.96$), and as the solvent quality improves T_{solid} drops substantially (about 30 °C in decane and another 20 °C in the decane in the presence of the small linear polymer chains).

Considering the effect of increasing the linear/star polymer size ratio, experiments with a linear polymer of 165000 g/mol (about the span molecular mass of the star) reveal that increasing the temperature has an appreciable influence on the star/linear mixture via an increase of the moduli and a change from a liquid-like mixture to a viscoelastic fluid. This eventually should bring about a glassy state, but presumably at temperatures beyond the experimentally used ones. In fact, in this particular case with a linear-to-star size ratio of about 0.5, the linear chains do not penetrate the stars but instead exert an osmotic force that tends to shrink them, as seen in Fig. 30 [301, 306] and Fig. 23b. The addition of linear chains has as a consequence an effective worsening of the solvent quality for the stars [306], shifting the glass transition temperature to high values. Extension is this work would provide the necessary information for the coarse-grained description of star/linear polymer mixtures in intermediate solvents [306].

9.2. Implications

The development of predictive tools based on appropriate star-star effective interaction potentials, will be an important step forward in our quest for designing and formulating soft colloidal composites with desired properties. It will also open the route for tailoring the rheology of such systems. Therefore, further experimental efforts in a wider range of linear-to-star size ratio (the crucial parameter) should have an impact. Moreover, there is always a concern of the presence of weak dispersion forces in these systems where the increase of temperature yields a better quality solvent. To this end, a connection with attractive glasses [59, 23, 87] may help revealing the universal aspects of glass formation and different glassy states in colloidal suspensions. Naturally, this last aspect applies to the problems discussed in sections 6, 7 and 8 as well.

10. CONCLUDING REMARKS AND OUTLOOK

Tailoring the flow of soft colloidal suspensions represents a grand rheological challenge. This, in turn, necessitates the proper description and control of the effective interactions in these systems. Undoubtedly, such a formidable task becomes complicated by the variety and the coupling of the interactions. This means that a good control of the particle interactions is needed. To this end, colloidal star polymers represent an ideal model soft colloidal system, amenable to experimental studies. They exhibit tunable, excluded volume (entropic) interactions, which can be described at a coarse-grained level with reasonable accuracy. Their structural and transport properties reflect the combination of polymeric and colloidal features. Of particular interest in this work is the behavior in the dense state and the possible manipulation of their rheology. There, these soft colloids become kinetically arrested and a variety of intriguing features of the glassy state are revealed. Based on the control parameters for monitoring these states, one can distinguish two situations:

(1) Upon heating, concentrated suspensions of colloidal stars in a solvent of intermediate quality undergo a reversible glass-like transition. This phenomenon is attributed to the increase of the stars effective volume fraction with temperature, leading to the formation of clusters and causing a kinetic arrest.

(2) The addition of linear or star polymers to a colloidal star glass brings about melting of the glass. Depletion is the origin of this effect and the control parameter is the additive-to-star size ratio (smaller than 1). Re-entrant glasses are formed up increasing depletion range (size ratio) or depletion strength (additive concentration).

Naturally, a combination of these two phenomena, e.g., thermal vitrification of star mixtures, reflects an interesting interplay of the swelling and depletion effects.

The above striking properties of soft colloids manifest the very nature of soft matter, i.e., the dramatic impact of weak external fields in inducing large macroscopic changes in this class of materials. Moreover, along with others, they can provide a ‘toolbox’ for the rational design and engineering of novel soft materials and the control of their rheology. To meet these challenges, several important problems need being addressed [201]. Here we only mention some interesting possibilities for further rheologically relevant investigations:

It is evident from this work with model colloidal star polymers, that it is possible to manipulate transitions in soft colloids with various thermal forces (temperature, solvent, depletion). This, in turn, provides the key for tailoring their rheology. There are still important open issues, such as the understanding of the re-entrant behaviour of star/linear polymer mixtures (and other soft colloid/polymer systems) in the protein limit, the possible re-entrant behaviour of the thermal soft colloidal glasses (preliminary studies are suggestive of this tendency, which brings analogies to the observations with the pluronic micelles [260]), the re-entrant glass in binary soft colloidal mixtures as the strength of depletion increases [333]. In the latter case, it is a prime importance to explore the different glassy states that may exist and understand their similarities and differences, as well as the rheological consequences of their presence. To this end, probing the high-freqency modulus of different solid-like soft colloidal systems is of great relevance, and may further yield novel material properties [335-337, 268, 269]. Along the same lines, a possible association of different glasses to fragile or ductile behaviour is of significance [32-34]. Of course, the number and length of the ‘grafted’ layers represents an additional parameter for softness, and thus rheology control [42, 210]. In this class of problems, the distinction between rheological (and other dynamic or structural) signatures of colloidal gels and glasses remains an ever challenging topic [270, 17, 232-234, 23, 271].

The discussion in this article was restricted to linear rheological response. There is a wide range of intriguing phenomena of immense scientific and technological interest, that relate to the nonlinear rheology of soft colloids. Some representative examples, drawn from the fragmental evidence with the model colloidal stars (but applicable to a wide range of soft colloids) include: (i) Yielding behaviour of the glasses: exploring the different mechanisms by which soft glasses melt under the influence of an external load, usually shear [61, 323, 338, 339]. To this end, a possible universal description of yielding in solid-like soft matter systems remains an open issue [340-347, 323, 327, 61, 328]. (ii) Aging of soft glasses and its relation to that of hard glasses [348-357], as well as its consequences on rheology [351, 352, 61, 358-360, 181]. (iii) Thixotropic behaviour [361-366]. (iv) Shear banding phenomena [367-371]. (v) Possible flow-induced structural changes in these deformable systems [76, 372, 371-373].

In closing, we hope that developments in this front with these model systems will be also valuable for assessing recent modelling approaches attempting at describing the rheological and dynamic properties of colloidal glasses [351, 356, 76, 368, 374-379].

ACKNOWLEDGEMENTS

Our current understanding of these systems is largely based on many enjoyable interactions over the past 10 years. We gratefully acknowledge fruitful collaborations with J. Roovers, C. N. Likos, G. Petekidis, G. Fytas, B. Loppinet, A. N. Beris, I. A. Bitsanis, P. T. Callaghan, C. Christopoulou, J. K. G. Dhont, G. Fleischer, N. Hadjichristidis, M. Helgeson, H. Iatrou, C. Mayer, G. Meier, S. Makrakis, K. Mortensen, T. Pakula, A. Rissanou, S. Rogers, A. N. Semenov, N. J. Wagner and E. Zaccarelli. We have also benefited a great deal from insightful discussions with M. E. Cates, M. Cloitre, R. H. Colby, J. F. Douglas, G. Gompper, K. Kremer, S. Kumar, H. Löwen, T. C. B. McLeish, J. Mewis, P. Pincus, P. N. Pusey, M. Ripol, W. B. Russel, J. Stellbrink, and A. Yodh. Part of this research has been supported by the European Union (HUSC network HPRN-CT2000-00017, Softcomp NoE NMP3-CT2004-502235).

REFERENCES

1. Jones, R. A. L., *Soft Condensed Matter*, Oxford University Press, New York (2002).
2. Hamley, I. W., *Introduction to Soft Matter*, Wiley, New York (2000).
3. Daoud, M, Williams C. E. (Eds.), *Soft Matter Physics*, Springer, Berlin, (1999).
4. Cates, M. E., Evans, M. R. (Eds.), *Soft and Fragile Matter. Nonequilibrium Dynamics, Metastability and Flow*, Institute of Physics Publishing, Bristol (2000).
5. Witten, T. A., *Structured Fluids*, Oxford University Press, New York (2004).
6. Rubinstein, M., Colby, R. H., *Polymer Physics*, Oxford University Press, New York (2003).
7. Larson, R. G., *The Structure and Rheology of Complex Fluids*, Oxford University Press, New York (1999).
8. Witten T. A., *Insights from soft condensed matter,* Rev. Mod. Phys. 71 (1999) S367-S373.
9. McLeish, T. (Ed.), *Theoretical Challenges in the Dynamics of Complex Fluids*, NATO ASI E339, Kluwer Academic Publishers, Amsterdam (1997).
10. de Gennes, P. G., Fragile Objects. Soft Matter, Hard Science and the Thrill of Discovery, Springer-Verlag, New York (1996).
11. Russel, W. B., Saville, D. A., Schowalter, W R, *Colloidal Dispersions*, Cambridge University Press: New York, (1989).
12. Von Grünberg, H. H., Colloidal suspensions – The classical model system for soft condensed matter physics, Adv. Solid State Phys., 42 (2002) 347-358.
13. Bandyopadhyay, R. Liang D., Harden J. L., Leheny R. L., *Slow dynamics, aging and glassy rheology in soft and living matter*, Solid State Commun., 139 (2006) 589-598.
14. Poon, W., McLeish, T., Donald, A., *Soft condensed matter: where physics meets biology*, Phys. World, May, (2001) 33-38.
15. Liu, A. J., Nagel, S. R., *Nonlinear Dynamics-Jamming is not Just Cool any More*, Nature, 396 (1998) 21.
16. Cates, M. E., Wittner, J. P., Bouchaud, J.-P., Claudin, P., *Jamming, Force Chains, and Fragile Matter*, Phys. Rev. Lett., 81 (1998) 1841-1844.
17. Trappe, V., Prasad V., Cipelletti L., Segre P.N,, Weitz D.A, *Jamming phase diagram for attractive particles*, Nature, 411 (2001) 772-775.
18. Liu, A. J., Nagel, S.R. (Eds.), Jamming and Rheology: Constrained Dynamics on Microscopic and Macroscopic Scales, Taylor and Francis: New York (2001).

19. Foffi, G., Sciortino, F., Tartaglia, P., Zaccarelli, E., Lo Verso, F., Reatto, L., Dawson, K. A., Likos, C. N., *Structural arrest in dense star-polymer solutions*, Phys. Rev. Lett., 90 (2003) 238301-1-4.

20. Prasad, V., Trappe, V., Dinsmore, A. D., Segre, P. N., Cipelletti, L., Weitz, D. A., *Universal Features of the Fluid to Solid Transition for Attractive Colloidal Particles*, Faraday Discuss., 123 (2003) 1-12.

21. Trappe, V., Sandkühler, P., *Colloidal gels – low density disordered solid-like states*, Curr. Opin. Colloid Interf. Sci., 8 (2004) 494-500.

22. Marty, G., Dauchot, O., *Subdiffusion and cage effect in a sheared granular material*, Phys. Rev. Lett., 94 (2005) 015701-4.

23. Sciortino, F., Tartaglia, P., *Glassy colloidal systems*, Adv. Phys., 54 (2005) 471-524.

24. Bender, J., Wagner, N. J., Reversible Shear thickening in monodisperse and bidisperse colloidal dispersions, J. Rheol., 40 (1996) 899-916.

25. Foss, D. R., Brady, J. F., Structure, diffusion and rheology of Brownian suspensions by Stokesian Dynamics simulation, J. Fluid Mech., 407 (2000) 167-200.

26. Maranzano, B. J., Wagner, N. J., The effects of interparticle interactions and particle size on reversible shear thickening: Hard-sphere colloidal dispersions, J. Rheol., 45 (2001) 1205-1222.

27. Melrose, J. R., Ball, R. C., Continuous shear thickening transitions in model concentrated colloids - The role of interparticle forces, J. Rheol., 48 (2004) 937-960.

28. Gopalakrishnan, V., Shah, S. A., Zukoski, C. F., *Cage melting and viscosity reduction in dense equilibrium suspensions*, J. Rheol., 49 (2005) 383-400.

29. Frith, W. J., d'Haene, P., Buscall, R., Mewis J., *Shear thickening in model suspensions of sterically stabilized particles*, J. Rheol., 40 (1996) 531-549.

30. Lee, Y. S., Wagner, N. J., Rheological Properties and Small-Angle Neutron Scattering of a Shear Thickening Nanoparticle Dispersion at High Shear Rates, Ind. Eng. Chem. Res., 45 (2006) 7015-7024.

31. Anderson, P. W., *Through the glass lightly*, Science, 267 (1995) 1615-1616.

32. Angell, C. A., Formation of glasses from liquids and biopolymers, Science, 267 (1995) 1924-1935.

33. Ediger, M. D., Angell, C. A., Nagel, S. R., *Supercooled liquids and glasses*, J. Phys. Chem., 100 (1996) 13200-13212.

34. Debenedetti P. G., Stillinger F. H., *Supercooled liquids and the glass transition*, Nature, 410 (2001) 259-267.

35. Götze, W., Aspects of Structural Glass transitions, in Hansen, J. P., Levesque, D., Zinn-Justin, J. (Eds.), *Liquids, Freezing and Glass Transition*, North-Holland, Amsterdam (1991).

36. Angell, C. A., Ngai, K. L., McKenna, G. B., McMillan, P. F.,, Martin, S. W., *Relaxation in glass forming liquids and amorphous solids*, J. Appl. Phys., 88 (2000) 3113.

37. Nommensen, P. A., Duits, M. H. G., van den Ende, D., Mellema, J., *Elastic Modulus at High Frequency of Polymerically Stabilized Suspensions*, Langmuir, 16 (2000) 1902-1909.

38. Mewis, J., Vermant J., *Rheology of sterically stabilized dispersions and lattices*, J., Prog. Organic Coatings, 40 (2000) 111-117.

39. Weiss, A., Dingenouts, N., Ballauff, M., Senff, H., Richtering, W., Comparison of the Effective Radius of Sterically Stabilized Latex Particles Determined by Small-Angle X-ray Scattering and by Zero Shear Viscosity, Langmuir, 14 (1998) 5083-5087.

40. Grest, G. S., Fetters, J. L., Huang, J. S., Richter, D., *Star Polymers: Experiment, Theory, and Simulation*, Adv. Chem. Phys. XCIV (1996) 67-163.

41. Roovers, J., Zhou, L.-L., Toporowski, P. M., van der Zwan, M., Iatrou, H.,, Hadjichristidis, N., *Regular star polymers with 64 and 128 arms. Models for polymeric micelles*, Macromolecules, 26 (1993) 4324-4331.

42. Likos, C. N., Effective interactions in soft condensed matter physics, Phys. Rep., 348 (2001) 267-439.

43. Vlassopoulos, D., Fytas, G., Pakula, T., Roovers, J., *Multiarm Star Polymers Dynamics*, J. Phys. Condens. Matter, 13 (2001) R855-R876.

44. Likos, C. N., Löwen, H., Watzlawek, M., Abbas, B., Jucknischke, O., Allgaier, J., Richter, D., *Star polymers viewed as ultrasoft colloidal particles*, Phys. Rev. Lett., 80 (1998) 4450.

45. Daoud, M., Cotton, J. P, *Star shaped polymers*, J. P., J. Phys. (Paris), 43 (1982) 531-538

46. Likos, C. N., *Soft matter with soft particles*, Soft Matter, 2 (2006) 478-498.

47. Semenov, A. N., Vlassopoulos, D., Fytas, G., Vlachos, G., Fleischer, G., Roovers J., *Dynamic Structure of Interacting Spherical Brushes*, Langmuir, 15 (1999) 358-368.

48. Kapnistos, M., Semenov, A. N., Vlassopoulos, D., Roovers, J., *Viscoelastic Response of Hyperstar Polymers in the Linear Regime*, J. Chem. Phys., 111 (1999) 1753-1759.

49. Pakula, T., Vlassopoulos, D., Fytas, G., Roovers, J., *Structure and Dynamics of Melts of Multiarm Polymer Stars*, Macromolecules, 31 (1998) 8931-8940.

50. Fleischer, G., Fytas, G., Vlassopoulos, D., Roovers, J.,, Hadjichristidis, N., *Self-Diffusion of Multiarm Star Polymers far from and near the Ordering Transition*, Physica A, 280 (2000) 266-278.

51. Doi, M., Edwards, S. F., *The Theory of Polymer Dynamics*, Oxford University Press, New York (1986).

52. Edwards, S. F., *The statistical mechanics of polymerized material*, Proc. Phys. Soc., 92 (1967) 9-13.

53. Edwards, S. F., *The theory of rubber elasticity*, Brit. Polym. J, 9 (1977) 140.

54. de Gennes, P. G., Reptation of a Polymer Chain in the Presence of Fixed Obstacles, J. Chem. Phys., 55 (1971) 572-579.

55. Pusey, P. N., van Megen, W., Phase behaviour of concentrated suspensions of nearly hard colloidal spheres, Nature 320 (1986) 340-342.

56. Pusey, P. N., *Colloidal Suspensions*, In: Hansen, J. P., Levesque, D., Zinn-Justin J. (Eds.), *Liquids, Freezing and Glass Transition*, North Holland: Amsterdam (1991).

57. Cohen, E. G., de Schepper, I. M., *Note on transport processes in dense colloidal suspensions*, J. Stat. Phys., 63 (1991) 241-248.

58. Frenkel J., *Kinetic Theory of Liquids*, Oxford, The Clarendon Press, (1946).

59. Pham, K. N., Puertas, A. M., Bergenholtz, J., Egelhaaf, S. U., Moussaid, A., Pusey, P. N., Schofield, A. B., Cates, M. E., Fuchs, M., Poon, W. C. K., *Multiple Glassy States in a Simple Model System*, Science, 296 (2002) 104.

60. Dawson, K. A., The glass paradigm for colloidal glasses, gels, and other arrested states driven by attractive interactions, Curr. Opin. Colloid Interf. Sci., 7 (2002) 218-227.

61. Helgeson, M. E., Wagner, N. J., Vlassopoulos, D., *Viscoelasticity and shear melting of colloidal star polymer glasses*, J. Rheol., 51 (2007) 297-316.

62. Halperin, A., Tirrell, M., Lodge T. P., *Tethered chains in polymer microstructures*, Adv. Polym. Sci., 100 (1992) 31-71.

63. Advincula, R. C., Brittain, W. J., Caster, K. C., Rühe J., *Polymer Brushes: Synthesis, characterization, Applications*, Wiley InterScience, New York (2004).

64. Reiter, G., Sommer, J.-U., *Crystallisation of adsorbed polymer monolayers*, Phys. Rev. Lett., 80 (1998) 3771-3774.

65. Michailidou, V., Loppinet, B., Prücker, O., Rühe, J., Fytas, G., *Cooperative Diffusion of End-Grafted Polymer Brushes in Good Solvents*, Macromolecules, 38 (2005) 8960.

66. Zhou, F., Huck, W. T. S., Surface grafted polymer brushes as ideal building blocks for “smart” surfaces, Phys. Chem. Chem. Phys., 8 (2006) 3815-3823.

67. Zhang, L.,, Granick, S., Interleaflet diffusion coupling when polymer adsorbs onto one sole leaflet of a supported phospholipid bilayer, Macromolecules, 40 (2007) 1366-1368.

68. Edmondson, S, Osborne, V. L., Huck, W. T. S., *Polymer brushes via surface-initiated polymerizations*, Chem. Rev., 33 (2004) 14-22.

69. Vincent, B., The preparation of colloidal particles having (post-grafted) terminally-attached polymer chains, Chemical Engineering Science, 48 (1993) 429-436.

70. Milling, A., Vincent, B., Emmett, S., Jones, A., Depletion flocculation in dispersions of sterically-stabilised silica particles 3. The effect of grafted chain coverage, Colloids and Surfaces, 57 (1991) 185-195.

71. de Kruif, C. G., Rouw, P. W., Briels, W. J., Duits, M. H. G., Vrij, A., May, R. P., Adhesive hard-sphere colloidal dispersion. A small angle neutron scattering study of stickiness and the structure factor, Langmuir, 5 (1989) 422-428.

72. Vrij, A., Philipse, A. P., Model particles for concentrated colloidal dispersions: From hard spheres to soft rods, In Pelizzetti, E. (ed.), Fine particles science and technology, Kluwer Academic Publishers, The Netherlands (1996).

73. Grant, M. C., Russel, W. B., *Volume-fraction dependence of elastic moduli and transition temperatures for colloidal silica gels*, Phys. Rev. E, 47 (1993) 2606–2614.

74. Chen, M., Russel, W. B., *Characteristics of flocculated silica dispersions,* J. Colloid Interface Sci., 141 (1991) 564-577.

75. Petekidis, G., Gapinski, J., Seymour, P., van Duijneveldt, J. S., Vlassopoulos, D., Fytas, G., *Dynamics of core-shell particles in concentrated suspensions*, Phys. Rev. E., 69 (2004) 042401-1-4.

76. Verduin, H., de Gans, B.J., Dhont, J.K.G., Shear induced structural changes in a gel-forming suspension by light scattering and rheology, Langmuir, 12 (1996) 2947.

77. Verduin, H., Dhont, J.K.G., *Phase diagram of a model adhesive hard-sphere dispersion*, J. Colloid Interface Sci., 172 (1995) 425.

78. Rueb, C. J., Zukoski, C. F., *Viscoelastic properties of colloidal gels*, J. Rheol., 41 (1997) 197-218.

79. Rueb, C. J., Zukoski, C. F., Rheology of suspensions of weakly attractive particles: Approach to gelation, J. Rheol., 41 (1997) 197-218.

80. Cawdery, N., Milling, A., Vincent, B., *Instabilities in dispersions of "hairy" particles on adding solvent-miscible polymers*, Colloids and Surfaces A: Physicochemical and Engineering Aspects, 86 (1994) 239-242

81. Nommensen, PA, Duits, MHG, van den Ende, D, Mellema, J, Steady shear behavior of polymerically stabilized suspensions: Experiments and lubrication based modeling, Phys. Rev. E, 59 (1999) 3147-3154.

82. Mewis, J., Biebaut, G., Shear thickening in steady and superposition flows effect of particle interaction forces, J. Rheol., 45 (2001) 799-813.

83. Mewis, J., Frith, W. J., Strivens, T. A., Russel, W. B., *The rheology of suspensions containing polymerically stabilized particles*, AIChE J., 35 (1989) 415-422.

84. Green, D.L., Mewis, J., Connecting the wetting and rheological behaviors of poly (dimethylsiloxane)-grafted silica spheres in poly(dimethylsiloxane) melts, Langmuir, 22 (2006) 9546-9553.

85. Hasegawa, R., Aoki, Y., Doi, M., *Optimum graft density for dispersing particles in polymer melts*, Macromolecules, 29 (1996) 6656-6662.

86. Castaing, J.C., Allain, C., Auroy, P., Auvray, L., *Rheology of nanosized hairy grain suspensions*, Eur. Phys. J. B, 10 (1999) 61-70.

87. Pham, K. N., Egelhaaf, S. U., Pusey, P. N., Poon, W. C. K., *Glasses in hard spheres with short range attraction*, Phys. Rev. E, 69 (2004) 011503-1-13.

88. Genz, U., Dagguano, B., Mewis, J., Klein, R., *Structure of sterically stabilized colloids*, Langmuir, 10 (1994) 2206-2212.

89. Cheng, Z., Phan, S.-E., Russel, W. B., Nature of the divergence in the low shear viscosity of dispersions of colloidal hard spheres, Phys. Rev. E, 65 (2002) 041405-1-8

90. Krishnamurthy, L., Wagner, N. J., The Influence of Weak Attractive Forces on the Microstructure and Rheology of Colloidal Dispersions, J. Rheol., 49 (2005) 475-499.

91. Krishnamurthy, L., *Microstructure and Rheology of Polymer-Colloid Mixtures*, Ph.D Thesis, University of Delaware, Newark, DE (2005).

92. Krishnamurthy, L., Mewis, J., Wagner, N. J., The effects of weak attractions on the zero shear viscosity of near hard sphere colloidal dispersion, J. Rheol. (2007), in press.

93. Raynaud, L., Ernst, B., Verge, C., Mewis, J., *Rheology of aqueous latices with adsorbed stabilizer layers*, J. Colloid Interface Sci, 181 (1996) 11-19.

94. Guo, X., Ballauff, M., Spatial dimensions of colloidal polyelectrolyte brushes as determined by dynamic light scattering, Langmuir, 16 (2000) 8719-8726.

95. Guo, X., Ballauff, M., Spherical polyelectrolyte brushes: Comparison between annealed and quenched brushes, Phys. Rev. E, 64 (2001) 051406.

96. Marra, A., Peuvrel-Disdier, E., Wittemann, A., Guo, X., Ballauff, M., *Rheology of dilute and semidilute suspensions of spherical polyelectrolyte brushes*, Colloid Polym. Sci., 281 (2003) 491-496.

97. Ballauff, M., Nanoscopic polymer particles with a well-defined surface: Synthesis, characterization, and properties, Macromol. Chem. Phys., 204 (2003) 220-234.

98. Ballauff, M., Borisov, O., *Polyelectrolyte brushes*, Curr. Opin. Colloid Interface Sci., 11 (2006) 316-323.

99. Rosenfeldt, S., Wittemann, A., Ballauff, M., Breininger, E., Bolze, J., Dingenouts, N., *Interaction of proteins with spherical polyelectrolyte brushes in solution as studied by small-angle x-ray scattering*, Phys. Rev. E, 70 (2004) 061403.

100. Wittemann, A., Ballauff, M., Interaction of proteins with linear polyelectrolytes and spherical polyelectrolyte brushes in aqueous solution, Phys. Chem. Chem. Phys., 8 (2006) 5269-5275.

101. Wittemann, A., Haupt, B., Ballauff, M., *Adsorption of proteins on spherical polyelectrolyte brushes in aqueous solution*, Phys. Chem. Chem. Phys., 5 (2003) 1671-1677.

102. Neumann, T., Haupt, B.and Ballauff, M., *High activity of enzymes immobilized in colloidal nanoreactors*, Macromolecular Bioscience, 4 (2004) 13-16.

103. Aoki, Y., Hatano, A., Watanabe, H., *Chain relaxation time in ABS polymer melts.* J. Soc. Rheol. Japan, 30 (2002) 59-63.

104. Aoki, Y., Hatano, A., Watanabe, H., *Nonlinear stress relaxation of ABS polymers in the molten state*, Macromolecules, 34 (2001) 3100-3107.

105. Fritz, G., Schadler, V., Willenbacher, N., Wagner, N.J., *Electrosteric stabilization of colloidal dispersions*, Langmuir 18 (2002) 6381-6390.

106. Shay, J. S., Raghavan, S. R, Khan, S. A. Thermoreversible gelation in aqueous dispersions of colloidal particles bearing grafted poly(ethylene oxide) chains, J. Rheol., 45 (2001) 913-927.

107. Zackrisson, M., Strasdner, A., Schurtenberger, P., Bergenholtz, J., *Structure, dynamics and rheology of concentrated dispersions of poly(ethylene glycol)-grafted colloids*, Phys. Rev. E 73 (2006) 011408-1-8

108. Bell, N. S., Piech, M., Photophysical effects between spirobenzopyran-methyl methacrylate-functionalized colloidal particles, Langmuir, 22 (2006) 1420-1427.

109. van Bruggen, M. P. B., Preparation and Properties of Colloidal Core-Shell Rods with Adjustable Aspect Ratios, Langmuir, 14 (1998) 2245 -2255.

110. Bourlinos, A. B., Chowdhurry, S. R., Jiang, D. D., An, Y. U., Zhang, Q., Archer, L. A., Giannelis, E. P., *Layered Organosilicate Nanoparticles with Liquidlike Behavior*, Small 1 (2005) 80-82.

111. Hamley, I. W., Nanoshells and nanotubes from block copolymers, Soft Matter, 1 (2005) 36-43.

112. Solomon, M. J., Boger, D. V., The rheology of aqueous dispersions of spindle-type colloidal hematite rods, J. Rheol., 42 (1998) 929-949.

113. Buining, P. A., Lekkerkerker, H. N. W., *Isotropic-nematic phase separation of a dispersion of organophilic boehmite rod*, J. Chem. Phys., 97 (1993) 11510-11516.

114. Dogic, Z., Philipse, A. P., Fraden, S., Dhont, J. K. G., *Concentraqtion-dependent sedimentation of colloidal rods*, J. Chem. Phys., 113 (2000) 8368-8377.

115. Krishnamoorti, R., Giannelis, E. P., *Rheology of end-tethered polymer layered silicate nanocomposites*, Macromolecules, 30 (1997) 4097-4102.

116. Zhang, Z. X., van Duijneveldt, J. S., *Isotropic-nematic phase transition of nonaqueous suspensions of natural clay rods*, J. Chem. Phys., 124 (2006) 154910-154916.

117. Islam, M. F., Alsayed, A. M., Dogic Z., Zhang J., Lubensky T. C., Yodh A. G., *Nematic nanotube gels*, Phys. Rev. Lett., 92 (2004) 088303-1-4.

118. Luckham, P. F., Rossi, S., *The colloidal and rheological properties of bentonite suspensions*, Adv. Colloid Interface Sci., 82 (1999) 43-92.

119. Krishnamoorti, R., Giannelis, E. P., *Strain hardening in model polymer brushes under shear*, Langmuir, 17 (2001) 1448-1452.

120. Dhont, J. K. G., Briels, W. J., *Viscoelasticity of suspensions of long, rigid rods*, Colloids Surf. A: Physicochem. Eng. Aspects, 213 (2003) 131.

121. Dhont, J. K. G., Briels, W. J., *Inhomogeneous suspensions of rigid rods in flow*, J. Chem. Phys., 118 (2003) 1466.

122. Halperin, A., *Polymeric micelles: a star model*, Macromolecules, 20 (1987) 2943-2946.

123. Förster, S., Wenz, E., Lindner, P., *Density Profile of Spherical Polymer Brushes*, Phys. Rev. Lett., 77 (1996) 95-98.

124. Gast, A. P., Structure, interactions, and dynamics in tethered chain systems, Langmuir, 12 (1996) 4060-4067.

125. Lund, R., Willner, L., Stellbrink, J., Lindner, P., Richter, D., *Logarithmic Chain-Exchange Kinetics of Diblock Copolymer Micelles*, Phys. Rev. Lett., 96 (2006) 068302-1-4.

126. Liu, G.J., *Nanostructures of Functional Block Copolymers*, Curr. Opin. Colloid Interface Sci., 3 (1998) 200-208.

127. Bang, J, Viswanathan, K, Lodge, TP, Park, MJ, Char, K, Temperature-dependent micellar structures in poly(styrene-b-isoprene) diblock copolymer solutions near the critical micelle temperature, J. Chem. Phys., 121 (2004) 11489-11496.

128. Mortensen, K., Structural studies of aqueous solutions of PEO-PPO-PEO triblock copolymers, their micellar aggregates and mesophases. A small-angle neutron scattering study, J. Phys.: Condens. Matter 8 (1996) 8 A103-A124.

129. Liu, G.J., *Polymeric Nanostructures*, in Handbook of Nanostructured Materials and Nanotechnology (H. S. Nalwa ed.), Academic Press: New York, volume 5 (1999) 475-500.

130. O'Reilly, R.K., Hawker, C.J., Wooley, K.L., Cross-linked block copolymer micelles: functional nanostructures of great potential and versatility, Chem. Soc. Rev., 35 (2006) 1068–1083.

131. Laurati, M., Stellbrink, J., Lund, R., Willner, L., Ricther, D., Zaccarelli, E., *Starlike micelles with starlike interactions:A quantitative evaluation of structure factors and phase diagram*, Phys. Rev. Lett., 94 (2005) 995504-1-4.

132. Munch, M. R., Gast, A. P., *Block copolymers at interfaces.1.Micelle Formation*, Macromolecules, 21 (1988) 1360-1366.

133. McConnell, G. A., Gast, A. P, Huang, J. C., Smith, S. D, *Disorder-order transitions in soft sphere polymer micelles*, Phys. Rev. Lett., 71 (1993) 2102-2105.

134. Ruzette, A. V., Leibler, L., *Block copolymers in tomorrow's plastics*, Nature Materials, 4 (2005) 19-31.

135. Cogan, K. A, Gast, A. P., Effect of water on diblock copolymers in oil: large aggregates, micelles, and microemulsions, Macromolecules, 23 (1990) 745-753.

136. Vagberg ,L. J. M., Cogan, K. A.,, Gast, A. P., *Light-scattering study of starlike polymeric micelles*, Macromolecules, 24 (1991) 1670-1677.

137. Cogan, K. A., Gast, A. P., Capel, M., *Stretching and scaling in polymeric micelles*, Macromolecules, 24 (1991) 6512-6520.

138. Lee, A. S., Bütün, V., Vamvakaki, M., Armes, S., Pople, J. A., Gast, A. P., *Structure of pH-dependent block copolymer micelles: Charge and ionic strength dependence*, Macromolecules, 35 (2002) 8540-8551.

139. Fernandez-Nieves, A., van Duijneveldt, J. S., Fernandez-Barbero, A., Vincent, B., de las Nieves, F. J., *Structure formation from mesoscopic soft particles*, Phy. Rev. E, 64 (2001) 051603.

140. Kimerling, A. S., Rochefort, W. E., Bhatia, S. R., *Rheology of block polyelectrolyte solutions and gels: A review*, Ind. Eng. Chem. Res., 45 (2006) 6885-6889.

141. McConnell, G. A., Gast, A. P., Melting of ordered arrays and shape transitions in highly concentrated diblock copolymer solutions, Macromolecules, 30 (1997) 435-444.

142. Liu, S. Y., Zhu, H., Zhao, H. Y., Jiang, M., Wu, C., Interpolymer hydrogen-bonding complexation induced micellization from polystyrene-b-poly(methyl methacrylate) and PS(OH) in toluene, Langmuir, 16 (2000) 3712-3717.

143. Xu, Z. S., Yi, C. F., Cheng, S. Y., Feng, L. X., Wu, C., *Study on solution properties of amphiphilic graft copolymer PMMA-g-PEO*, Acta Polymerica Sinica, 6 (2000) 701-706.

144. Alexandridis, P., Athanassiou, V., Hatton, T. A., Pluronic-P1O5 PEO-PPO-PEO Block Copolymer in Aqueous Urea Solutions: Micelle Formation, Structure, and. Microenvironment, Langmuir, 11 (1995) 2442-2450.

145. Lin, Y. N., Alexandridis, P., Cosolvent effects on the micellization of an amphiphilic siloxane graft copolymer in aqueous solutions, Langmuir, 18 (2002) 4220-4231.

146. Yang, L, Alexandridis, P, Steytler, DC, Kositza, MJ, Holzwarth, JF, Small-angle neutron scattering investigation of the temperature-dependent aggregation behavior of the block copolymer pluronic L64 in aqueous solution, Langmuir, 16 (2000) 8555-8561.

147. Alexandridis, P., Olsson, U., Lindman, B., Structural polymorphism of amphiphilic copolymers: Six lyotropic liquid crystalline and two solution phases in a poly(oxybutylene)-b-poly(oxyethylene)-water-xylene system, Langmuir, 13 (1997) 23-34.

148. Alexandridis, P., Olsson, U., Lindman, B., A record nine different phases (four cubic, two hexagonal, and one lamellar lyotropic liquid crystalline and two micellar solutions) in a ternary isothermal system of an amphiphilic block copolymer and selective solvents (water and oil), Langmuir, 14 (1998) 2627-2638.

149. Ivanova, R., Lindman, B., Alexandridis, P., Effect of glycols on the self-assembly of amphiphilic block copolymers in water. 1. Phase diagrams and structure identification, Langmuir, 16 (2000) 3660-3675.

150. Ivanova, R., Lindman, B., Alexandridis, P., Evolution in structural polymorphism of pluronic F127 poly(ethylene oxide)-poly(propylene oxide) block copolymer in ternary systems with water and pharmaceutically acceptable organic solvents: From "glycols" to "oils", Langmuir, 16 (2000) 9058-9069.

151. Watanabe, H., *Rheology of diblock copolymer micellar systems*, Acta Polym., 48 (1997) 215-233.

152. Watanabe, H., Kanaya, T., Takahashi, Y., *Equilibrium elasticity of diblock copolymer micellar lattice*, Macromolecules, 34 (2001) 662-665.

153. Sato, T., Watanabe, H., Osaki, K., Rheological and dielectric behaviour of styrene-isoprene-styrene triblock copolymer in n-tetradecane: 1. Rubbery-plastic-viscous transition, Macromolecules, 29 (1996) 3890-3897.

154. Sato, T., Watanabe, H., Osaki, K., *Thermoreversible physical gelation of block copolymers in selective solvent*, Macromolecules, 33 (2000) 1686-1691.

155. Corte, L., Yamauchi, K., Court, F., Cloitre, M., Hashimoto, T., Leibler, L., *Annealing and defect trapping in lamellar phases of triblock terpolymers*, Macromolecules, 36 (2003): 7695-7706.

156. Yamaguchi, D., Cloitre, M., Panine, P., Leibler, L., Phase behavior and viscoelastic properties of thermoplastic elastomer gels based on ABC triblock copolymers, Macromolecules, 38 (2005) 7798-7806.

157. Boudet, C., Iliopoulos, I., Poncelet, O., Cloitre, M., Control of the chemical cross-linking of gelatin by a thermosensitive polymer: Example of switchable reactivity, Biomacromolecules, 6 (2005) 3073-3078.

158. Laflèche, F., Durand, D., Nicolai, T., Association of Adhesive Spheres Formed by Hydrophobically End-Capped PEO. 1. Influence of the Presence of Single End-Capped PEO, Macromolecules, 36 (2003) 1331-1340.

159. Pham, Q. T., Russel, W. B., Thibeault, J. C., Lau, W., Micellar Solutions of Associative Triblock Copolymers: Entropic Attraction and Gas-Liquid Transition, Macromolecules, 32 (1999) 2996-3005.

160. Pham, Q. T., Russel, W. B., Thibeault, J. C., Lau, W., Micellar Solutions of Associative Triblock Copolymers: The relationship between structure and rheology, Macromolecules, 32 (1999) 5139-5146.

161. Pozzo, D. C., Hollabaugh, K. R., Walker, L. M., *Rheology and phase behavior of copolymer-templeted nanocomposite materials*, J. Rheol., 49 (2005) 759-782.

162. Yan X.H., Liu G.J., Li. Z., Preparation and Phase Separation of Block Copolymer Nanotube Multiblocks, J. Am. Chem. Soc. 126 (2004) 10059-66.

163. Yan X.H., Liu G.J., Preparation, Characterization, and Solution Viscosity of Polystyrene-block-polyisoprene Nanofiber Fractions, Langmuir, 20 (2004) 4677-4683.

164. Angelopoulos S. A., Tsitsilianis C., Thermo-Reversible Hydrogels Based on Poly(N,N-diethylacrylamide)-block-poly(acrylic acid)-block-poly(N,N-diethylacrylamide) Double Hydrophilic Triblock Copolymer, Macromol. Chem. & Phys, 207 (2006) 2188-2194.

165. Bossard F., Aubry T., Gotzamanis G. T., Tsitsilianis C., pH-Tunable rheological properties of a telechelic cationic polyelectrolyte reversible hydrogel, Soft Matter, 2 (2006) 510-516.

166. Bütün V., Liu S., Weaver J.V.M., Bories-Azeau X., Cai Y., Armes S.P., *A brief review of 'schizophrenic' block copolymers,* Reactive and Functional Polymers, 66 (2006) 157-165.

167. Discher, D. E., Kamien, R. D., *Towards precision micelles*, Nature, 430 (2004) 519-520.

168. Mountrichas, G., Mpiri, M., Pispas, S., Micelles of star block (PSPI)8 and PSPI diblock copolymers (PS=polystyrene, PI=polyisoprene): Structure and kinetics of micellization, Macromolecules, 38 (2005) 940-947.

169. Murray, M. J., Snowden, M. J., *The preparation, characterization and applications of colloidal mcrogels*, Adv. Colloid Interface Sci. 54 (1995) 73.

170. Antionetti, M., Rosenauer, C., *Properties of fractal divinylbenzene microgels*, Macromolecules, 24 (1991) 3434-3442.

171. Okay, O., Funke, W., *Steric Stabilization of Reactive Microgels from 1,4-Divinylmenzene*, Makromol. Chem. Rapid Commun. 11 (1990) 583-587.

172. Saito, R., Ishizu, K., *Flower type microgels: 1. Synthesis of the microgels*, Polymer, 38 (1997) 225-229.

173. Heskins, M., Guillet, J. E., *Solution properties of poly (N–isopropylacrylamide,* J. Macromol. Sci. Chem., 8 (1968) 1444.

174. Wiedemair, J., Serpe, M. J., Kim, J., Masson, J. F., Lyon, L. A., Mizaikoff B., Kranz C., *In-situ AFM studies of the phase-transition behavior of single thermoresponsive hydrogel particles*, Langmuir 23 (2007) 130-137.

175. Rodriquez, B. E., Wolfe, M. S., Fryd, M., *Nonuniform Swelling of Alkali Swellable Microgels*, Macromolecules, 27 (1994) 6642-6647.

176. Hu, T., Wu, C., *Clustering induced collapse of a polymer brush*, Phys. Rev. Lett., 83 (1999) 4105-4108.

177. Borrega, R., Cloitre, M., Betremieux, I., Ernst, B., Leibler, L., Concentration dependence of the low-shear viscosity of polyelectrolyte micro-networks: From hard spheres to soft microgels, Europhys. Lett., 47 (1999) 729-735.

178. Buscall, R., An effective hard-sphere model of the non-Newtonian viscosity of stable colloidal dispersions: Comparison with further data for sterically stabilised latices and with data for microgel particles, Colloid Surf. A: Physicochemical and Engineering Aspects, 83 (1994) 33-42.

179. Paulin, S. E., Ackerson, B. J., Wolfe,, M. S., *Equilibrium andshear induced nonequilibrium phase behaviour of PMMA microgel spheres*, J. Colloid Interface Sci., 178 (1996) 251-262.

180. Paulin, S. E., Ackerson, B. J., Wolfe, M. S., *Microstructure-dependent viscosity in concentrated suspensions of soft spheres*, Phys. Rev. E, 55 (1998) 5812-5819.

181. Cloitre, M, Borrega, R, Leibler, L, *Rheological Aging and Rejuvenation in Microgel Pastes*, Phys. Rev. Lett., 85 (2000) 4819-4822.

182. Meeker, SP, Bonnecaze, RT, Cloitre, M, *Slip and flow in soft particle pastes*, Phys. Rev. Lett., 92 (2004) 198302-1-4.

183. Dingenouts, N, Norhausen, C, Ballauff, M, Observation of the volume transition in thermosensitive core-shell latex particles by small-angle X-ray scattering, Macromolecules, 31 (1998) 8912-8917.

184. Seelenmeyer, S., Deike, I., Rosenfeldt, S., Norhausen, C., Dingenouts, N., Ballauff, M., Narayanan, T., Lindner, P., *Small-angle x-ray and neutron scattering studies of the volume phase transition in thermosensitive core-shell colloids*, J. Chem. Phys., 114 (2001) 10471-10478.

185. Senff, H, Richtering, W., Temperature sensitive microgel suspensions: Colloidal phase behavior and rheology of soft spheres, J. Chem. Phys., 111 (1999) 1705-1711.

186. Senff, H., Richtering, W. Influence of cross-link density on rheological properties of temperature-sensitive microgel suspensions, Colloid Polym. Sci., 278 (2000) 830-840.

187. Saunders, BR, Vincent, B, Microgel particles as model colloids: theory, properties and applications, Adv. Colloid Interf. Sci., 80 (1999) 1-25.

188. Berndt, I., Pedersen, J.S., Richtering, W., *Temperature-sensitive core-shell microgel particles with dense shell*, Angew. Chem. 45 (2006) 1737 – 1741.

189. Berndt, I., Popescu, C., Wortmann, F.-J., Richtering, W., *Mechanics versus Thermodynamics: Swelling in Multi-Temperature Sensitive Core-ShellMicrogels*, Angew. Chem. 45 (2006) 1081 – 1085.

190. Stieger, M., Pederson, J. S., Lindner, P., Richtering, W., Are thermoresponsive microgels model systems for concentrated colloidal suspensions? A rheology and small-angle neutron scattering study, Langmuir, 20 (2004) 7283-7292.

191. Kim, JH, Ballauff, M, The volume transition in thermosensitive core-shell latex particles containing charged groups, Colloid Polym. Sci., 277 (1999) 1210-1214.

192. Berndt, I, Richtering, W. *Doubly temperature sensitive core-shell microgels,* Macromolecules 36 (2003) 8780-8785.

193. Crassous, JJ, Ballauff, M, Drechsler, M, Schmidt, J, Talmon, Y, Imaging the volume transition in thermosensitive core-shell particles by cryo-transmission electron microscopy, Langmuir, 22 (2006) 2403-2406.

194. Senff, H, Richtering, W, Norhausen, C, Weiss, A, Ballauff, M, *Rheology of a temperature sensitive core-shell latex*, Langmuir, 15 (1999) 102-106.

195. Crassous, JJ, Siebenburger, M, Ballauff, M, Drechsler, M, Henrich, O, Fuchs, M, Thermosensitive core-shell particles as model systems for studying the flow behavior of concentrated colloidal dispersions, J. Chem. Phys., 125 (2006) 204906-11.

196. Deike, I, Ballauff, M, Rheology of thermosensitive latex particles including the high-frequency limit, J. Rheol., 45 (2001) 709-720.

197. Berndt, I., Pedersen, J. S., Richtering, W., *Structure of Multiresponsive "Intelligent" Core-Shell-Microgels,* J. Am. Chem. Soc. 127 (2005) 9372 – 9373.

198. Lambeth, R. H., Ramakrishnan, S., Mueller, R., Poziemski, J. P., Miguel, G. S., Markoski, L. J., Zukuski, C. F., Moore J. S., *Synthesis and aggregation behavior of thermally responsive star polymers*, Langmuir, 22 (2006) 6352-6360.

199. Mackay, M. E., Dao, T. T., Tuteja, A., Ho, D. L., Horn, B. V., Kim, H-C., Hawker, C. J., *Nanoscale effects leading to non-Einstein-like decrease in viscosity*, Nature Materials, 2 (2003) 762-766.

200. Charalabidis, D., Pitsikalis, M., Hadjichristidis, N., Model linear and star-shaped polyisoprenes with phosphatidylcholine analogous end-groups. Synthesis and association behavior in cyclohexane, Macromol. Chem. Phys., 203, (2002) 2132-2141.

201. Vlassopoulos, D., Colloidal star polymers: models for studying dynamically arrested states in soft matter, J. Polym. Sci.: Part B: Polym. Phys., 42 (2004) 2931-2941.

202. Zhou, L.-L., Hadjichristidis, N., Toporowski, P. M., Roovers J., *Synthesis and properties of regular star polybutadienes with 32 arms*, Rubber Chem. Techn., 65 (1992) 303-314.

203. Toporowski, P. M., Roovers, J., *Synthesis and properties of eighteen-arm polybutadienes*, J. Polym. Sci., Polym. Chem. Ed., 24 (1986) 3009–3019.

204. Tande, B. M., Wagner, N. J., Mackay, M. E., Hawker, C. J., Jeong, M., Viscosimetric, *Hydrodynamic, and Conformational Properties of Dendrimers and Dendrons*, Macromolecules, 34 (2001) 8580-8585.

205. Ballauff, M., Likos, C. N., *Dendrimers in Solution: Insight from Theory and Simulation,* Angew. Chem. Int. Ed., 43 (2004) 2998–3020.

206. Roovers, J., Toporowski, P., Martin, J., *Synthesis and characterization of multiarm star polybutadienes* Macromolecules, 22 (1989) 1897-1903.

207. Stellbrink, J., Allgaier, J., Richter, D., *Dynamics of star polymers: Evidence for a structural glass transition*, Phys. Rev. E, 56 (1997) R3772-R3775.

208. Yamamoto, T., *Studies of Long Time Relaxation of Multi-Arm Star Polymers*, Ph.D Thesis, Kyoto University, Kyoto, Japan (2003).

209. Ishizu, K., Ono, T., Uchida, S., *Superlattice formation on star polymer solutions*, J. Colloid Interface Sci., 192 (1997) 189-193.

210. Vlassopoulos, D., Fytas, G., Pispas, S., Hadjichristidis, N., *Spherical polymeric brushes viewed as soft colloidal particles: zero-shear viscosity*, Physica B, 296, (2001) 184-189.

211. Stiakakis, E., Vlassopoulos, D., Loppinet, B., Roovers, J., Meier, G., Kinetic *Arrest of Crowded Soft Spheres in Solvents of Varying Quality*, Phys. Rev. E., 66 (2002) 051804-1-9.

212. Loppinet, B., Stiakakis, E., Vlassopoulos, D., Fytas, G., Roovers, J., *Reversible Thermal Gelation in Star Polymers: An Alternative Route to Jamming of Soft Matter*, Macromolecules, 34 (2001) 8216-8223.

213. Segre, P. N., Meeker, S. P., Pusey, P. N., Poon, W. C. K., *Viscosity and Structural Relaxation in Suspensions of Hard-Sphere Colloids*, Phys. Rev. Lett., 75 (1995) 958-961.

214. Phan, S.-E., Russel, W. B., Cheng, Z., Zhu, J., Chaikin, P. M., Dunsmuir, J. H., Ottewill, R. H., *Phase transition, equation of state, and limiting shear viscosities of hard sphere dispersions*, Phys. Rev. E., 54 (1996) 6633-6645.

215. Roovers, J., Concentration-dependence of the relative viscosity of star polymers, Macromolecules, 27 (1994) 5359-5364.

216. Brady, F., Model hard-sphere dispersions: statistical mechanical theory, simulations, and experiments, Curr. Opin. Colloid Interface Sci. 1 (1996) 472.

217. Witten, T. A., Pincus, P. A., Cates, M. E., *Macrocrystal ordering in star-polymer solutions*, Europhys. Lett., 2 (1986) 137-140.

218. Witten, T. A., Pincus, P. A., *Colloid stabilization by long grafted polymers*, Macromolecules, 19 (1986) 2509-2513.

219. Watzlawek, M., Likos, C. N., Löwen, H., *Phase diagram of star polymer solutions*, Phys. Rev. Lett., 1999, 82, 5289-5292.

220. Watzlawek, M., *Phase Behaviour of Star Polymers*, Ph.D Thesis, University of Düsseldorf, Shaker Verlag: Aachen, Germany (2000).

221. Willner, L., Jucknischke, O., Richter, D., Roovers, J., Zhou, L.-L., Toporowski, P. M., Fetters, L. J., Huang, J. S., Lin, M. Y., Hadjichristidis, N., *Structural Investigation of Star Polymers in Solution by Small-Angle Neutron Scattering*, Macromolecules, 27 (1994) 3821-3829.

222. Richter, D., Jucknischke, O., Willner, L., Fetters, L. J., Lin, M., Huang, J. S., Roovers, J., Toporovski, C., Zhou, L. L., *Scaling properties and ordering phenomena of star polymers in solution*, J. Phys. IV, C8 (1993) 3-12.

223. Willner, L., Jucknischke, O., Richter, D., Farago, B., Fetters, L. J., Huang, J. S., *Ordering phenomena of star polymers in solution by SANS*, Europhys. Lett., 19 (1992) 297-303.

224. Jucknischke, O. *Untersuchung der Struktur von Sternpolymeren in Loesung mit Neutronenkleinwinkelstreung*, Münster, Germany, Westfälischen Wilhelms-Universität, PhD thesis (1995).

225. Kapnistos, M., Vlassopoulos, D., Fytas, G., Mortensen, K., Fleischer, G., Roovers, J., *Reversible Thermal Gelation in Soft Spheres*, Phys. Rev. Lett., 85 (2000) 4072-4075.

226. Fischer, E. W., Light scattering and dielectric studies on glass forming liquids, Physica A, 201 (1993) 183-202.

227. Vasin, M. G., Lad'yanov, V. I., A description of Fischer cluster formation in supercooled liquids within the framework of the continuous theory of defects, J. Phys.: Condens. Matter, 17 (2005) S1287-S1292.

228. Kanaya, T., Patkowski, A., Fischer, E. W., Seils, J. Glaser, H., Kaji, K., *Light scattering studies on long-range density fluctuations in a glass-forming polymer*, Acta Polymer., 45 (2003) 137-142.

229. Rissanou, A. N., Vlassopoulos, D., Bitsanis, I. A., Thermal Vitrification in Suspensions of "Soft Colloids": Molecular Dynamics Simulations and Comparison with Experiments, Phys. Rev. E., 71 (2005) 011402-1-12.

230. Härtl, W., *Colloidal Glasses*, Curr. Opin. Colloid Interface Sci., 2001, 6, 479.

231. Puertas, A. M., Fuchs, M., Cates, M. E., *Comparative Simulation Study of Colloidal Gels And Glasses*, Phys. Rev. Lett., 88 (2002) 098301.

232. Salaniwal, S., Kumar, S. K., Douglas, J. F., *Amorphous Solidification in Polymer-Platelet Nanocomposites*, Phys. Rev. Lett., 89 (2002) 258301.

233. Kumar, S. K., Douglas, J. F., *Gelation in Physically Associating Polymer Solutions*, Phys. Rev. Lett., 87 (2001) 188301.

234. Donati, C., Glotzer, S. C., Poole, P. H., Kob, W., Plimpton, S. J., *Spatial correlations of mobility and immobility in a glass-forming Lennard-Jones liquid*, Phys. Rev. E., 60 (1999) 3107-3119.

235. Gohr, K., Pakula, T., Tsutsumi, K., Schärtl, W., *Dynamics of Copolymer Micelles in an Entangled Homopolymer Matrix*, Macromolecules, 32 (1999) 7156-7165.

236. Hamley, I. A., Daniel, C., Mingvanish, W., Mai S-M., Booth, C., Messe, L., Ryan, A. J., From Hard Spheres to Soft Spheres: The Effect of Copolymer Composition on the Structure of Micellar Cubic Phases Formed by Diblock Copolymers in Aqueous Solution, Langmuir, 16 (2000) 2508-2514.

237. Buitenhuis, J., Förster, S., Block copolymer micelles: Viscoelasticity and interaction potential of soft spheres, J. Chem. Phys., 107 (1997) 262-272.

238. Lodge, T. P., Bang, J., Hanley, K. J., Krocak, J., Dahlquist, S., Sujan, B., Ott, J., Origins *of Anomalous Micellization in Diblock Copolymer Solutions*, Langmuir, 19 (2003) 2103-2109.

239. Lai, C., Russel, W. B., Register, R. A., Scaling of Domain Spacing in Concentrated Solutions of Block Copolymers in Selective Solvents, Macromolecules, 35 (2002) 4044-4049.

240. Pispas, S., Hadjichristidis, N., Micellization Behavior of Poly(butadiene-b-sodium methacrylate) Copolymers in Dilute Aqueous Media, Macromolecules, 36 (2003) 8732-8737.

241. Zhang, G., Winnik, F. M., Wu, C., Structure of a Collapsed Polymer Chain with Stickers: A Single- or Multiflower?, Phys. Rev. Lett., 90 (2003) 035506.

242. Mallamace, F., Chen, S.-H., Liu, Y., Lobry, L., Micali, N., *Percolation and viscoelasticity of triblock copolymer micellar solutions*, Physica A, 266 (1999) 123-135.

243. Alexandridis, P., *Amphiphilic copolymers and their applications*, Curr. Opin. Colloid Interface Sci., 1 (1996) 490-501.

244. Bhatia, S. R., Mourchid, A., Joanicot, M., *Block copolymer assembly to control fluid rheology*, Curr. Opin. Colloid Interface Sci., 6 (2001) 471-478.

245. Loppinet, B., Sigel, R., Larsen, A., Fytas, G., Vlassopoulos, D., Liu, G., *Structure and Dynamics in Dense Suspensions of Micellar Nanocolloids*, Langmuir, 16 (2000) 6480-6484.

246. Likos, C. N., Löwen, H., Poppe, A., Willner, L., Roovers, J., Cubitt, B., Richter, D., *Ordering phenomena of star polymer solutions approaching the Θ state*, Phys. Rev. E, 80 (1998) 6299-6307.

247. Götze, W., Recent tests of the mode-coupling theory for glassy dynamics, J. Phys. Condens. Matter, 11 (1999) A1-A45.

248. Götze, W., Sjogren, L., Comments on the mode coupling theory for structural relaxation, Chem. Phy., 212 (1996) 47-59.

249. Kob, W.,*Computer simulations of supercooled liquids and glasses*, J. Phys.: Condens. Matter, 11 (1999) R85-R115.

250. Callaghan, P.T., Coy, A., MacGowan, D., Packer, K.J., Zelaya, F.O., *Diffraction-like effects in NMR diffusion studies of fluids in porous solids*, Nature, 351 (1991) 467-469.

251. Ahlstrom, B., Bergenholtz, J., Prediction of structures and gel transitions in systems of colloids with moderate-range attractions, J. Phys. Condens. Matter, 19 (2007) 036102.

252. Lo Verso, F., Reatto, L., Foffi, G., Tartaglia, P., Dawson, K. A., Star polymers: *A study of the structural arrest in the presence of attractive interactions*, Phys. Rev. E., 70 (2004) 061409-1-13.

253. Lo Verso, F., Likos, C. N., Mayer, C., Reatto, L., *Effect of attraction on the dynamical arrest of soft colloids*, Mol. Phys., 104 (2006) 3523-3534

254. Sztucki, M., Narayanan, T., Belina, G., Moussaid, A., Pignon, F., Hoekstra, H., *Kinetic arrest and glass-glass transition in short-ranged attractive colloids*, Phys. Rev. E, 74 (2006) 051504-1-12.

255. Plazanet, M., Johnson, M.R., Schweins, R., Trommsdorff, H. P., *Inverse freezing in alpha-cyclodextrin solutions probed by quasi elastic neutron scattering*, Chem. Phys., 331 (2006) 35-41.

256. Missirlis, D., Hubbell, J.A., Tirelli, N., *Thermally-induced glass formation from hydrogel nanoparticles*, Soft Matter 2 (2006) 1067-1075.

257. Battaglia, G., Ryan, A.J., *The evolution of vesicles from bulk lamellar gels*, Nature Materials, 4 (2005) 869-876.

258. Foreman, M.B., Coffman, J.P., Murcia, M.J., Cesana, S., Jordan, R., Smith, G. S., Naumann, C. A., Gelation of amphiphilic lipopolymers at the air-water interface: 2D analogue to 3D gelation of colloidal systems with grafted polymer chains?, Langmuir, 19 (2003) 326-332.

259. Loyen, K., Iliopoulos, I., Audebert, R., Olsson, U., Reversible thermal gelation in polymer/surfactant systems. Control of the gelation temperature, Langmuir, 11 (1995) 1053-1056.

260. Mallamace, F., Broccio, M., Tartaglia, P., Chen, W. R., Faraone, A., Chen, S. H., *Viscoelastic processes in non-ergodic states (percolation and glass transitions) of attractive micellar systems*, Physica A, 330 (2003) 206-217.

261. Chen, S.H., Chen, W.R., Mallamace, F., The glass-to-glass transition and its end point in a copolymer micellar system, Science, 300 (2003) 619-622.

262. Chen, S.-H., Chen, W.-R., Mallamace, F., Observation of liquid-to-glass and glass-to-glass transitions in L64/D2O triblock copolymer micellar system, Molecular Simul., 29 (2003) 611-618

263. Perahia, D., Traiphol, R., Bunz, U., From single molecules to aggregates to gels in dilute solution: Self-organization of nanoscale rodlike molecules, J. Chem. Phys., 117 (2002) 1827-1832.

264. Versteegen, R. M., van Beek, D. J. M., Sijbesma, R.P., Vlassopoulos, D., Fytas, G., Meijer, E. W., *Dendrimer-based transient supramolecular networks,* J. Am. Chem. Soc., 127 (2005) 13862-13868.

265. Glotzer, S.C., Solomon, M.J., Kotov, N., *Self-assembly: from nanoscale to microscale colloids*, AIChE Journal, 50 (2004) 2978-2985.

266. Winter, H. H., Mours, M., *Rheology of polymers near liquid-solid transitions*, Adv. Polym Sci 134 (1997) 165-234.

267. Mason, T. G., Weitz, D. A., Linear Viscoelasticity of Colloidal Hard Sphere Suspensions near the Glass Transition, Phys. Rev. Lett., 75 (1995) 2770-2773.

268. Ozon, F., Petekidis, G. , Vlassopoulos, D., *Signatures of Nonergodicity Transition in a Soft Colloidal System*, invited article, Ind. Eng. Chem. Res., 45 (2006) 6946-6952.

269. Bhatia, S. R., Mourchid, A., Gelation of micellar block polyelectrolytes: Evidence of glassy behavior in an attractive system, Langmuir, 18 (2002) 6469-6472.

270. Segre, P. N., Prasad, V., Schofield, A. B., Weitz, D. A., *Glasslike kinetic arrest at the colloidal-gelation transition*, Phys. Rev. Lett., 86 (2001) 6042-6045.

271. Manley, S., Wyss, H. M., Miyazaki, K., Conrad, J. C., Trappe, V., Kaufman, L. J., Reichman, D. R., Weitz, D. A., *Glasslike arrest in spinodal decomposition as a route to colloidal gelation*, Phys. Rev. Lett., 95 (2005) 238302-1-4.

272. Brady, J. F., The rheological behavior of concentrated colloidal dispersions, Journal of Chemical Physics, 99 (1993) 567-581.

273. Wagner, N. J., the high-frequency modulus of colloidal suspensions and the effects of hydrodynamic interactions, J. Colloid Interface Sci., 161 (1993) 169-181

274. van Hooy-Corstjens C.S.J., Hohne G.W.H., Rastogi S., *Inverse melting in syndiotactic polystyrene*, Macromolecules, 38 (2005) 1814 – 1821.

275. van Ruth, N.J.L., Rastogi, S., Nonlinear changes in specific volume: a route to resolve entropy crisis, Macromolecules 37 (2004) 8191 – 8194.

276. Tammann, G. *Kristallisieren and Schmelzen*, Metzger und Wittig, Leipzig, Germany (1903).

277. Stiakakis, E., Kapnistos, M., Vlassopoulos, D., unpublished data (2007).

278. Asakura, S., Oosawa, F., On interaction between 2 bodies immersed in a solution of macromolecules, J. Chem. Phys., 22 (1954) 1255-1256.

279. Asakura, S., Oosawa, F., Interaction between particles suspended in solutions of macromolecules, J. Polym. Sci., 33 (1958) 183-192.

280. Vrij, A., Polymers at interfaces and interactions in colloidal dispersions, Pure Appl. Chem., 48 (1976) 471-483.

281. Gast, A. P., Hall, C. K., Russel, W. B.*, Polymer induced phase separations in nonaqueous colloidal suspensions*, J. Colloid Interface Sci., 96 (1983) 251-267.

282. Gast, A. P., Russel, W. B., Hall, C. K., An experimental and theoretical study of phase transitions in the polystyrene latex and hydroxyethylcellulose system, J. Colloid Interface Sci., 109 (1986) 161-171.

283. Patel, P. D., Russel, W. B., An experimental study of aqueous suspensions containing dissolved polymer. Part B: Rheology, J. Colloid Interface Sci., 131 (1989) 201-210.

284. Lekkerkerker, H. N. W., Poon, W. C. K., Pusey, P. N., Stroobants, A., Warren, P. B., *Phase-behavior of colloid plus polymer mixtures*, Europhys. Lett., 20 (1992) 559-564.

285. Meijer, E. J., Frenkel, D., *Colloids dispersed in polymer-solutions – A computer-simulation study*, J. Chem. Phys., 100 (1994) 6873-6887.

286. Ramakrishnan, S., Fuchs, M., Schweizer, K.S., Zukoski, C.F., *Entropy driven phase transitions in colloid-polymer suspensions: Tests of depletion theories*, J. Chem. Phys., 116 (2001) 2201-2212.

287. Bolhuis, P. G., Louis, A. A., Hansen, J-P., Influence of Polymer-Excluded Volume on the Phase-Behavior of Colloid-Polymer Mixtures, Phys. Rev. Lett., 89 (2001) 128302.

288. Tuinier, R., Rieger, J., de Kruif, C. G., *Depletion-induced phase separation in colloid-polymer mixtures*, Adv. Colloid Interface Sci., 103 (2003) 1-31.

289. Hunter, R. J., *Foundations of colloid science*, 2nd Ed., Oxford University Press: New York, (2001).

290. Poon, W. C. K., Phase separation, aggregation and gelation in colloid-polymer mixtures and related systems, Curr. Opin. Colloid Interface Sci., 3 (1998) 593-599.

291. Poon, W. C. K., Egelhaaf, S. U., Stellbrink, J., Allgaier, J., Schofield, A. B., Pusey, P. N., *Beyond simple depletion: phase behaviour of colloid-star polymer mixtures*, Phil. Trans. R. Soc. Lond. A, 359 (2001) 897-907.

292. Dzubiella, J., Jusufi, A., Likos, C. N., von Ferber, C., Löwen, H., Stellbrink, J., Allgaier, J., Richter, D., Schofield, A. B., Smith, P. A., Poon, W. C. K., Pusey, P. N., *Phase separation in star polymer-colloid mixtures*, Phys. Rev. E 64 (2001) R010401-1-4.

293. Dzubiella, J., Likos, C. N., Lowen, H., *Star polymers as depleting agents of colloidal hard spheres*, Europhys. Lett., 58 (2002) 133-138.

294. Stiakakis, E., Vlassopoulos, D., Likos, C. N., Roovers, J., Meier, G., *Polymer-Mediated Melting in Ultrasoft Colloidal Gels*, Phys. Rev. Lett., 89 (2002) 208302.

295. Ketz, R. J., Prud'homme, R. K., Graessley, W. W., *Rheology of concentrated microgel solutions*, Rheol. Acta, 27 (1988) 531-539.

296. Crassous, J. J., Regisser, R., Ballauff, M,, Willenbacher, N., Characterization of the viscoelastic behavior of complex fluids using the piezoelectric axial vibrator, J. Rheol., 49 (2005) 851-863.

297. Stiakakis, E., Petekidis, G., Vlassopoulos, D., Likos, C. N., Iatrou, H., Hadjichristidis, N., Roovers, J., *Depletion and cluster formation in soft colloid-polymer mixtures*, Europhys. Lett., 72 (2005) 664-670.

298. Poon, W. C. K., *The physics of a model colloid-polymer mixture*, J. Phys.: Condens. Matter, 14 (2002) R859-R880.

299. Bartsch, E., Eckert, T., Pies, C., Sillescu, H., *The effect of free polymer on the glass transition dynamics of microgel colloids*, J. Non-Cryst. Solids, 307 (2002) 802-811.

300. Dawson, K. A., Foffi, G., Fuchs, M., Götze, W., Sciortino, F., Sperl, M., Tartaglia, P., Voigtmann, Th., Zaccarelli, *Higher-order glass-transition singularities in colloidal systems with attractive interactions*, Phys. Rev. E, 63 (2000) 011401.

301. Stiakakis, E., Vlassopoulos, D., Roovers, J., *Thermal Jamming in Colloidal Star-Linear Polymer Mixtures*, Langmuir, 19 (2003) 6645-6649.

302. Likos, C. N., Mayer, C., Stiakakis, E., Petekidis, G., *Clustering of soft colloids due to polymer additives*, J. Phys.: Condens. Matter 17 (2005) S3363-S3369.

303. Archer, A. J., Likos, C. N., Evans, R., *Binary star-polymer solutions: bulk and interfacial properties*, J. Phys.: Condens. Matter, 14 (2002) 12031-12050.

304. Wu, J., Liu, Y., Chen, W.-R., Cao, J., Chen, S.-H., *Structural arrest transitions in fluids described by two Yukawa potentials*, Phys. Rev. E, 70 (2004) 050401-1-4.

305. Sciortino, F., Mossa, S., Zaccarelli, E., Tartaglia, P., Equilibrium cluster phases and low-density arrested disordered states: the role of short-range attraction and long-range repulsion, Phys. Rev. Lett., 93 (2004) 055701-1-4.

306. Mayer, C., Likos, C. N., *A coarse-grained description of star-linear polymer mixtures*, Macromolecules, 40 (2007) 1196-1206.

307. Campell, A. I., Anderson, V. J., van Duijneveldt, J. S., Bartlet,t P., *Dynamical arrest in attractive colloids: the effect of long-range repulsion*, Phys. Rev. Lett., 94 (2005) 208301-1-4.

308. Mutch, K. J., van Duijneveldt, J. S., Eastoe J., *Colloid-polymer mixtures in the protein limit*, Soft Matter, 3 (2007) 155-167.

309. Bolhuis, P. G., Meijer, E. J., Louis, A. A., *Colloid-polymer mixtures in the protein limit*, Phys. Rev. Lett., 90 (2003) 068304-1-4.

310. Kulkarni, A. M., Chatterjee, A. P., Schweizer, K. S., Zukoski, C. F., *Depletion Interactions in the Protein Limit: Effects of Polymer Density Fluctuations*, Phys. Rev. Lett., 83 (1999) 4554-4557.

311. Otsubo, Y., Umeya, K., Rheological properties of silica suspensions in polyacrylamide solutions, J. Rheol., 28 (1984) 95-108.

312. Eckert, T., Bartsch, E., Re-entrant glass transition in a colloid-polymer mixture with depletion attractions, Phys. Rev. Lett., 701 (2002) 89 (2002) 125701-1-4.

313. Zaccarelli, E., Foffi, G., Dawson, K. A., Buldyrev, S. V., Sciortino, F., Tartaglia, P., *Confirmation of anomalous dynamic arrest in attractive colloids: a molecular dynamics study*, Phys. Rev. E, 66 (2002) 041402-1-11.

314. Cracium, L., Carreau, P. J., Heuzey, M.-C., van de Ven, T. G. M., Moan, M., *Rheological properties of concentrated latex suspensions of poly(styrene-butadiene)*, Rheologica Acta, 42 (2003) 410-420.

315. Eckert, T., Bartsch, E., Glass transition dynamics of hard sphere like polystyrene microgel colloids with short-ranged attractions, J. Phys.: Condens. Matter, 16 (2004) S4937-S4950.

316. Foffi, G., Dawson, K. A., Buldyrev, S. V., Sciortino, F., Zaccarelli, E., Tartaglia, P., *Evidence for an unusual dynamical-arrest scenario in short-ranged colloidal systems*, Phys. Rev. E, 65 (2002) 050802-1-4.

317. Miller, M. A., Frenkel, D., *Phase diagram of the adhesive hard sphere fluid*, J. Chem. Phys., 121 (2004) 535-545.

318. Poon, W. C. K., Pirie, A. D., Pusey, P. N., *Gelation in colloid-polymer mixtures*, Farday Discuss., 101 (1995) 65-76.

319. Evans, R. M. L., Poon, W. C. K., Diffusion evolution of stable and metastable phases. II. Theory of nonequilibrium behavior in colloid-polymer mixtures, Phys. Rev. E, 56 (1997) 5748-5758.

320. Zaccarelli, E., Mayer, C., Asteriadi, A., Likos, C. N., Sciortino, F., Roovers, J., Iatrou, H., Hadjichristidis, N., Tartaglia, P., Löwen, H., Vlassopoulos, D., *Tailoring the Flow of Soft Glasses*, Phys. Rev. Lett., 95 (2005) 268301-4.

321. Mayer, C., Stiakakis, E., Zaccarelli, E., Likos, C. N., Sciortino, F., Tartaglia, P., Löwen, H., Vlassopoulos, D., *Rheological Transitions in Asymmetric Colloidal Star Mixtures*, Rheol. Acta, 46 (2007) 611-619.

322. von Ferber, C., Jusufi, A., Watzlawek, M., Likos, C. N., Lowen, H., *Polydisperse star polymer solutions*, Phys. Rev. E., 62 (2000) 6949-6956.

323. Petekidis, G., Vlassopoulos, D., Pusey, P. N., *Yielding and flow of colloidal glasses*, Farday Discuss., 123 (2003) 287-302.

324. Götze, W., Voigtmann, T., Effect of composition changes on the structural relaxation of a binary mixture, Phys. Rev. E., 67 (2003) 021502.

325. Barrat, J. L., Latz, A., *Mode-coupling theory for the glass-transition in a simple binary mixture*, J. Phys.: Condens. Matter, 2 (1999) 4289-4295.

326. Imhof, A., Dhont, J. K. G., Experimental phase diagram of a binary colloidal hard-sphere mixture with a large size ratio, Phys. Rev. Lett., 75 (1995) 1662-1665.

327. Pham, K. N., Petekidis, G., Egelhaaf, S. U., Pusey, P. N., Vlassopoulos, D., Poon, W. C. K., *Yielding in Colloidal Glasses*, Europhys. Lett. 75 (2006) 624-630.

328. Chen, W.-R., Mallamace, F., Glinka, C. J., Fratini, E., Chen, S.-H., Neutron- and light-scattering studies of the liquid-to-glass transitions in dense copolymer micellar solutions, Phys. Rev. E, 68 (2003) 041402-1-15.

329. Grandjean, J., Mourchid, A., Re-entrant glass transition and logarithmic decay in a jammed micellar system. Rheology and dynamics investigation, Europhys. Lett., 65 (2004) 712-718

330. Grandjean, J., Mourchid, A., Entropic attraction and fluid-glass transition in micellar solutions of associative diblock copolymers, Phys. Rev. E, 72 (2005) 041503-1-8

331. Narayanan, T., Sztucki, M., Belina, G., Pignon, F., *Microstructure and rheology near an attractive colloidal glass transition*, Phys. Rev. Lett., 96 (2006) 258301-1-4.

332. Sciortino, F., *One liquid, two glasses*, Nature Mater., 1(2002) 145-146.

333. Mayer, C., Vitrification mechanisms in soft colloidal mixtures, PhD thesis, Univ. of Düsseldorf, Germany 2007.

334. Frankel, D., *Playing tricks with designer atoms*, Science, 296 (2002) 65-66.

335. Penciu, R. S., Fytas, G., Economou, E. N., Steffen, W., Yannopoulos, S. N., *Acoustic Excitations in Suspensions of Soft Colloids*, Phys. Rev. Lett., 85 (2000) 4622-4625.

336. Penciu, R. S., Kriegs, H., Petekidis, G., Fytas, G., Economou, E. N., *Phonons in colloidal systems*, J. Chem. Phys., 118 (2003) 5224-5240.

337. Cheng, W., Wang, J. J., Jonas, U., Fytas, G., Stefanou, N., *Observation and tuning of hypersonic bandgaps in colloidal crystals*, Nature Materials, 5 (2006) 830-836.

338. Petekidis, G., Vlassopoulos, D., Pusey, P. N., *Yielding and Flow in Sheared Colloidal Glasses*, J. Phys.: Condens. Matter, 16 (2004) S3955-S3963.

339. Petekidis, G., Carrier, V., Non-linear rheology of colloidal glasses of soft core-shell particles, submitted to J. Rheol.

340. Hyun, K., Kim, S. H., Ahn, K. H., Lee, S. J., *Large amplitude oscillatory shear as a way to classify the complex fluids*, Journal of Non-Newtonian Fluid Mechanics 107(2002) 51-65.

341. Miyazaki, K., Wyss, H. M., Weitz, D. A., Reichman, D. R., *Nonlinear viscoelasticity of metastable complex fluids*, Europhys. Lett. 75 (2006) 915-921.

342. Moller, P. C. F., Mewis, J., Bonn, D., Yield stress and thixotropy: on the difficulty of measuring yield stresses in practice, Soft Matter, 2 (2006) 274-283.

343. Kobelev, V., Schweizer, K. S., Dynamic yielding, shear thinning, and stress rheology of polymer-particle suspensions and gels, J. Chem. Phys. 123 (2005) 164903.

344. Rouyer, F., Cohen-Addad, S., Hohler, R., *Is the yield stress of aqueous foam a well-defined quantity?*, Colloids and Surfaces a-Physicochemical and Engineering Aspects 263 (2005) 111-116.

345. Baxter-Drayton, Y., Brady, J. F., Brownian electrorheological fluids as a model for flocculated dispersions, J. Rheol., 40 (1996) 1027-1056

346. Grant, M., Russel, W. B., Distinguishing slip and dynamic yielding in a weakly flocculated colloidal dispersion, Coll. Surf. A, 161 (2000) 271-280.

347. Kobelev, V., Schweizer, K. S. *Nonlinear elasticity and yielding of depletion gels*, J. Chem. Phys. 123 (2005) 164902-1-13

348. Cipelletti, L., Manley, S., Ball, R. C., Weitz, D. A., *Universal Aging Features in the Restructuring of Fractal Colloidal Gels*, Phys. Rev. Lett., 84 (2000) 2275-2278.

349. Cipelletti, L., Ramos, L., *Slow dynamics in glassy soft matter*, J. Phys. Condens. Matter, 17 (2005) R253-R285.

350. Ramos, L., Cipelletti, L., Intrinsic aging and effective viscosity in the slow dynamics of a soft glass with tunable elasticity, Phys. Rev. Lett., 94 (2005) 158301-1-4

351. Ajdari, A., Mechanical aging and non-linear rheology of concentrated colloidal suspensions: experimental facts and simple models, In Barrat, J.-L., Feigelman, M. and Kurchan, J.(eds), Slow relaxations and nonequilibrium dynamics in condensed matter, EDP Sciences- Springer Verlag, Berlin, Germany (2003)

352. Sollich, P., *Soft Glassy Rheology*, In Weiss, R. G., Terech, P. (eds), *Molecular Gels. Materials with Self-Assembled Fibrillar Netwroks*, Springer, The Netherlands (2006)

353. Cloitre, M, Borrega, R, Monti, F, Leibler, L, *Glassy dynamics and flow properties of soft colloidal pastes*, Phys. Rev. Lett., 90 (2003) 068303.

354. Mazoyer, S., Cipelletti, L., Ramos, L., *Origin of the slow dynamics and the aging of a soft glass*, Phys. Rev. Lett., 97 (2006) 238301-1-4.

355. Purnomo, EH, van den Ende, D, Mellema, J, Mugele, F. *Linear viscoelastic properties of aging suspensions*. Europhys. Lett., 76 (2006) 74-80.

356. Fielding, S. M., Sollich, P., Cates, M. E., *Aging and rheology in soft materials*, J. Rheol., 44 (2000) 323-369.

357. Brader, J. M., Voigtmann, Th., Cates, M. E., Fuchs, M., *Dense Colloidal Suspensions under Time-Dependent Shear*, Phys. Rev. Lett., 98 (2007) 058301.

358. Derec, C., Ajdari, A., Lequeux, F., *Rheology and aging : A simple approach*, Eur. Phys. J. E., 4 (2001) 355-361.

359. Derec, C., Ducouret, G., Ajdari, A., Lequeux, F., Aging and nonlinear rheology in suspensions of polyethylene oxide-protected silica particles, Phys. Rev. E., 67 (2003) 061403-1-9.

360. Viasnoff, V., Jurine, S., Lequeux, F., *How are colloidal suspensions that age rejuvenated by strain application?,* Farday Discuss., 123 (2003) 253-266.

361. Mewis, J., *Thixotropy - General-Review*, Journal of Non-Newtonian Fluid Mechanics, 6 (1979) 1-20.

362. Dullaert, K., Mewis, J., *Thixotropy: Build-up and breakdown curves during flow*, J. Rheol., 49 (2005) 1213-1230.

363. Dullaert, K., Mewis, J., *A structural kinetics model for thixotropy*, J. Non-Newtonian Fluid Mech., 139 (2006) 21-30

364. Dullaert, K., Mewis, J., *A model system for thixotropy studies*, Rheol. Acta, 45 (2005) 23-32

365. Coussot, P., Nguyen, Q. D., Huynh, H. T., Bonn, D., *Viscosity bifurcation in thixotropic, yielding fluids*, J. Rheol., 46 (2002) 573-589

366. Mujumdar, A., Beris, A. N., Metzner, A. B., *Transient phenomena in thixotropic systems*, J. Non-Newtonian Fluid Mech., 102 (2002) 157-178

367. Holmes, W. M., Callaghan, P. T., Vlassopoulos, D., Roovers, J., *Shear Banding Phenomena in Ultrasoft Colloidal Glasses*, J. Rheol., 48 (2004) 1085-1102.

368. Fielding, S., Olmsted, P., Spatio-temporal oscillations and rheochaos in a simple model of shear banding, Phys. Rev. Lett., 92 (2004) 084502.)

369. Dhont, J.K.G., Lettinga, M.P., Dogic, Z., Lenstra, T.A.J., Wang, H., Rathgeber, S., Carletto, P., Willner, L., Frielinghaus, H., Lindner, P., *Shear-banding and microstructure of colloids in shear flow*, Faraday Discuss., 123 (2003) 157-172.

370. Kang, K., Lettinga, M.P., Dogic, Z., Dhont, J.K.G., *Vorticity banding in rodlike virus suspensions*, Phys. Rev. E., 74 (2006) 026307-1-12

371. Vermant, J., Solomon, M.J., *Flow induced structure in colloidal suspensions*, J. Phys.: Condens. Matter. 17 (2005) R187-R216.

372. Ripoll, M. Winkler, R. G., Gompper, G., *Star polymers in shear flow*. Phys.Rev. Lett., 96 (2006) 188302-1-4.

373. Gadala-Maria, F., Acrivos, A., Shear-induced structure in a concentrated suspension of solid spheres, J. Rheol., 24 (1980) 799-814.

374. Holmes, C. B., Cates, M. E., Fuchs, M., Sollich, P., *Glass transitions and shear thickening suspension rheology*, J. Rheol., 49 (2005) 237-269.

375. Sollich, P., Rheological Constitutive Equation for a Model of Soft Glassy Materials, Phys. Rev. E, 58 (1998) 738-759.

376. Fuchs, M., Cates, M. E., *Schematic models for dynamic yielding of sheared colloidal glasses*, Faraday Discuss. 123 (2003) 267-286.

377. Lacevic, M., Glotzer, S. C., *Dynamical heterogeneity and jamming in glass-forming liquids*, J. Phys. Chem. B 108 (2004) 19623-19633

378. Dudowicz, J., Freed, K. F., Douglas, J. F., *Lattice model of living polymerization: I. Basic thermodynamic properties*, J. Chem. Phys. 111 (1999) 7116-7127.

379. Allegrini, P., Douglas, J. F., Glotzer, S. C., Dynamic entropy as a measure of caging and persistent particle motion in supercooled liquids, Phys. Rev. E 60 (1999) 5714-5723.

380. Baig, C., Jiang, B., Edwards, B.J., Keffer, D.J., Cochran, H.D., *A comparison of simple rheological models and simulation data of n-hexadecane under shear and elongational flow*, J. Rheol., 50 (2006) 625-640.

381. Mavrantzas, V.G., Theodorou, D.N., *Atomistic Monte Carlo simulation of steady-state uniaxial, elongational flow of long-chain polyethylene melts: dependence of the melt degree of orientation on stress, molecular length and elongational strain rate*, Macromol. Theory Simul., 9 (2000) 500-515.

